Reviews in Mineralogy & Geochemistry
Vol. 55, pp. 65-111, 2004

Applying Stable Isotope Fractionation Theory to New Systems

Edwin A. Schauble

Department of Earth and Space Sciences
University of California, Los Angeles
Los Angeles, California 90095-1567, U.S.A.

INTRODUCTION

A basic theoretical understanding of stable isotope fractionations can help researchers plan and interpret both laboratory experiments and measurements on natural samples. The goal of this chapter is to provide an introduction to stable isotope fractionation theory, particularly as it applies to mass-dependent fractionations of non-traditional elements and materials. Concepts are illustrated using a number of worked examples. For most elements, and typical terrestrial temperature and pressure conditions, equilibrium isotopic fractionations are caused by the sensitivities of molecular and condensed-phase vibrational frequencies to isotopic substitution. This is explained using the concepts of vibrational zero-point energy and the partition function, leading to Urey's (1947) simplified equation for calculating isotopic partition function ratios for molecules, and Kieffer's (1982) extension to condensed phases. Discussion will focus on methods of obtaining the necessary input data (vibrational frequencies) for partition function calculations. Vibrational spectra have not been measured or are incomplete for most of the substances that Earth scientists are interested in studying, making it necessary to estimate unknown frequencies, or to measure them directly. Techniques for estimating unknown frequencies range from simple analogies to well-studied materials to more complex empirical force-field calculations and *ab initio* quantum chemistry. Mössbauer spectroscopy has also been used to obtain the vibrational properties of some elements, particularly iron, in a variety of compounds. Some kinetic isotopic fractionations are controlled by molecular or atomic translational velocities; this class includes many diffusive and evaporative fractionations. These fractionations can be modeled using classical statistical mechanics. Other kinetic fractionations may result from the isotopic sensitivity of the activation energy required to achieve a transition state, a process that (in its simplest form) can be modeled using a modification of Urey's equation (Bigeleisen 1949).

Theoretical estimates of isotopic fractionations are particularly powerful in systems that are difficult to characterize experimentally, or when empirical data are scarce. The accuracy of a theoretical calculation is limited by uncertainty in input data, and by errors resulting from simplified thermodynamic treatment of molecular motion. Typical uncertainties are larger than the nominal precision of a careful isotope ratio measurement, although ongoing improvements in the quality of spectroscopic data and molecular modeling methods are helping to close this gap. Nonetheless, the accuracy of relatively simple theoretical models is sufficient to provide a quantitative framework for interpreting the results of a set of measurements. Theoretical calculations are easily extended to temperature conditions that are not easily accessed by experiments, which is especially relevant for low-temperature mineral-solution fractionations where isotopic exchange equilibrium often cannot be achieved on a reasonable laboratory

1529-6466/04/0055-0003$05.00

time scale. Qualitative rules of thumb based on theoretical concepts can be applied to systems that have not been explicitly studied. Complex fractionations, involving a combination of mechanisms, are common, and theoretical techniques can provide a unique perspective to help pick apart the underlying causes of an observed fractionation, and help understand and demonstrate its geochemical significance.

Overview

The purpose of this chapter is to provide a brief, practical guide to the theory of stable isotope fractionations. This subject is particularly apt for inclusion in a volume dedicated to less studied and novel stable isotope systems, because these systems often lack an extensive record of measurements and empirical intuitions to guide the planning and interpretation of analytical campaigns. As technological advances like multiple collector inductively coupled plasma mass spectrometry (MC-ICP-MS) push stable isotope geochemistry into uncharted territory, it becomes increasingly necessary for analysts—as well as interested researchers outside of the field of stable isotope geochemistry—to have an informed perspective on the basic mechanisms driving variations in isotopic abundances in natural samples.

This review will introduce basic techniques for calculating equilibrium and kinetic stable isotope fractionations in molecules, aqueous complexes, and solid phases, with a particular focus on the thermodynamic approach that has been most commonly applied to studies of equilibrium fractionations of well-studied elements (H, C, N, O, and S) (Urey 1947). Less direct methods for calculating equilibrium fractionations will be discussed briefly, including techniques based on Mössbauer spectroscopy (Polyakov 1997; Polyakov and Mineev 2000).

History

The theory of stable isotope fractionation precedes the development of modern mass spectrometry, and includes a few very early studies (Lindemann and Aston 1919; Lindemann 1919; Urey and Greiff 1935). The modern theoretical formulation for calculating equilibrium isotope fractionations can be credited to seminal work by Urey (1947) and Bigeleisen and Mayer (1947), which forms the basis for much of this chapter. Theoretical calculations in these papers successfully predicted the directions, magnitudes, and temperature sensitivities of isotopic fractionations. These calculations suggested the possibility of paleothermometry using $^{18}O/^{16}O$ fractionation in the calcite-water system (Urey 1947), foreshadowing the creation of a major field of geochemical research. Later the Urey formulation was extended to encompass crystals and some amorphous solids (e.g., Bottinga 1968; Kieffer 1982). A key point is that all of these theoretical treatments result from a simplified thermodynamic model of the quantum mechanics of molecular vibration and rotation—making theoretical calculations feasible for many important substances—while retaining enough accuracy to be quantitatively useful. As we will see, limited or imprecise data on molecular or crystal vibrations are a major issue to be overcome in calculating accurate theoretical fractionations. Several excellent reviews of stable isotope fractionation theory applied to the commonly studied elements—H, C, N, O, and S—are available in the literature (Richet et al. 1977; O'Neil 1986; Criss 1991, 1999; Chacko et al. 2001).

There have been relatively few theoretical studies of fractionations involving other elements. Lindemann (1919) probably performed the first theoretical calculation of a stable isotope fractionation, estimating the vapor pressures of the isotopes of lead. Urey (1947) and Urey and Greiff (1935) modeled equilibrium isotope fractionations for several geochemically important molecules containing chlorine, bromine, and iodine. Bigeleisen and Mayer (1947) briefly discuss possible fractionations involving the silicon and tin halides, focusing specifically on the effect of coordination number on fractionations. Later theoretical work was concentrated in the specialized literature of isotope separation. Of particular interest during this period was the development of force-field and quantum-mechanical techniques

for estimating unknown vibrational frequencies of molecules containing rare isotopes (Kotaka and Kakihana 1977; Kotaka et al. 1978; Hanschmann 1984). In recent years, as the set of elements with detectable natural isotopic variations has expanded, theoretical estimates of isotopic fractionations for boron (Oi 2000; Oi and Yanase 2001), lithium (Yamaji et al. 2001), chlorine (Paneth 2003; Schauble et al. 2003), chromium (Schauble et al. in press) and iron (Polyakov 1997; Polyakov and Mineev 2000; Schauble et al. 2001, Anbar et al. in press) have been published.

General rules governing equilibrium stable isotope fractionations

It is clear, from an examination of both observed and theoretically calculated isotope fractionations, that there are a number of qualitative chemical rules that can be used to estimate which substances will tend to be enriched in heavy isotopes in a given geochemical system. O'Neil (1986) tabulated five characteristics that are shared by the elements that show large variations in isotopic composition in nature. These include (i) low atomic mass, (ii) large relative mass differences between stable isotopes, (iii) tendency to form highly covalent bonds, (iv) multiple oxidation states or other chemical variability, and (v) availability of multiple isotopes with sufficient abundance to make measurements feasible. The elements covered in the present volume, in general, fail to meet one or more of these criteria. They are heavy (i.e., Fe, Mo, and Cd), do not have large mass differences between the measured stable isotopes (Cr), form bonds that are predominantly ionic (Li, Mg, Ca) rather than covalent, or have homogenous chemistry and a single predominant oxidation state in nature (Li, Mg, Si, Ca). Nonetheless, these rules are strongly supported by theoretical considerations originally derived by Bigeleisen and Mayer (1947), and form the basis for a qualitative guide to stable isotope fractionations in all elements:

Qualitative Rules governing equilibrium stable isotope fractionations:

1. Equilibrium isotopic fractionations usually decrease as temperature increases, roughly in proportion to $1/T^2$ for most substances. Note that exceptions may occur, particularly if the fractionation is very small, or if the element of interest is bonded directly to hydrogen in one phase.
2. All else being equal, isotopic fractionations are largest for light elements and for isotopes with very different masses, scaling roughly as $(m_{heavy} - m_{light})/(m_{light}m_{heavy})$ (often simplified to $\Delta m/m^2$) where m_{light} and m_{heavy} are the masses of two isotopes of an element, Δm is the difference between their masses, and m is the average atomic mass of the element.
3. At equilibrium, the heavy isotopes of an element will tend to be concentrated in substances where that element forms the stiffest bonds (i.e., bonds with high spring constants). The magnitude of the isotopic fractionation will be roughly proportional to the difference in bond stiffness between the equilibrated substances. Bond stiffness is greatest for *short*, *strong* chemical bonds; these properties correlate with:
    a. high oxidation state in the element of interest
    b. for anions like Cl^- and Se^{2-} (and O^{2-}), high oxidation state in the atoms to which the element of interest is bonded
    c. bonds involving elements near the top of the periodic table
    d. the presence of highly covalent bonds between atoms with similar electronegativities
    e. for transition elements, low-spin electronic configurations, also d^3 or d^8 electronic structure for octahedrally-coordinated atoms
    f. low coordination number

4. Substances where the element of interest is directly bonded to hydrogen, or is part of a low-mass molecule, may not be as enriched in heavy isotopes as would be expected from rule (3). This phenomenon, usually of 2nd order importance, is most pronounced for substances with stiff bonds and at low temperatures.

Rules (2) and (3) imply that large equilibrium fractionations are most likely to occur at low temperatures between substances with markedly different oxidation states, bond partners, electronic configurations, or coordination numbers.

It is important to point out that these rules (particularly 3 and 4) are largely untested with respect to fractionations in the less-well studied elements (those other than H, C, N, O, and S) at the present time. Furthermore, within rule (3), it is not known which chemical properties are the most important determinants of bond stiffness. The order of listing reflects a rough estimate of relative importance, based on experiments and theoretical studies in a variety of isotopic systems. However, this order is likely to vary somewhat from one system to another even if it is generally correct. What is known is that measurable isotopic fractionations are typically larger and more common in samples from low-temperature environments than in high-temperature (particularly igneous) environments for Ca (Russell et al. 1978; Skulan et al. 1997), Fe (Beard et al. 2003), Mo (Barling et al. 2001), and Mg (Galy et al. 2002). $^{56}Fe/^{54}Fe$ ratios are higher in aqueous Fe^{3+} than in coexisting aqueous Fe^{2+} (rule 3a) (Johnson et al. 2002), and Fe^{3+}-Cl^- complexes retained on ion-exchange resins appear to have lower $^{56}Fe/^{54}Fe$ ratios than Fe^{3+}-OH_2 complexes in solution (rules 3b and 3c) (Roe et al. 2003). Borate solutions with low pH, favoring the 3-coordinate $B(OH)_3$ have a greater affinity for heavy ^{11}B than high pH solutions dominated by 4-coordinated $[B(OH)_4]^-$ (rule 3f) (Kakihana et al. 1977). Clearly, more experiments are needed before a robust assessment of these rules can be made.

These rules suggest that stable isotope measurements of redox-active transition elements (e.g., Cr, Fe, Cu and Mo), and main group elements (Cl, Br, and Te) are likely to provide records of modern and ancient oxidation conditions. For chalcophile and siderophile elements like Fe, Cu, Zn, and Mo, low and moderate temperature partitioning between oxide, sulfide, and/or metal phases is also likely to cause diagnostic isotopic fractionation. In contrast, isotopic fractionation of main group lithophile metals like Li, Mg, Si and Ca are more likely to reflect changes in coordination number. Equilibrium fractionations in this last group (particularly for the heavier elements) are likely to be rather small, and may commonly be overwhelmed by kinetic fractionations in low-temperature and biological systems.

Kinetic isotope fractionations also show systematic behavior, although they are more difficult to describe with a list of widely applicable rules. Here the term kinetic is being used loosely to describe a host of basically one-directional processes occurring under conditions of incomplete isotopic exchange. This definition is useful in its simplicity, although it encompasses a number of distinct fractionation mechanisms, and in practice there is some ambiguity in dealing with "equilibrium-like" fractionations (like oxygen-isotope fractionation in biologically precipitated calcite). One common feature in many kinetic fractionations is that light isotopes, being more reactive, are concentrated in reaction products. This behavior is observed, for instance, in rapid precipitations of Fe^{3+} oxyhydroxide and oxide minerals from Fe^{3+}-bearing solutions (Bullen et al. 2001; Skulan et al. 2002), in evaporation of many substances including silicate melts (Davis et al. 1990), and in numerous biological reactions. Diffusive and evaporative kinetic fractionations do not, in general, decrease in magnitude with increasing temperature in the same way that equilibrium fractionations do (although they may be sensitive to temperature). Kinetic fractionations are usually sensitive to a host of factors (such as reaction rates and the presence of exchange catalysts) in addition to temperature.

Fractionation factors

Before introducing the quantitative theory of isotope fractionations, it will be useful to review terms relevant to calculating fractionation factors.

The isotope fractionation factor for isotopes ${}^{light}X$ (light) and ${}^{heavy}X$ (heavy) between two substances *XA* and *XB* is usually expressed in terms of "α":

$$\alpha_{XA\text{-}XB} = \frac{\left({}^{heavy}X \big/ {}_{light}X\right)_{XA}}{\left({}^{heavy}X \big/ {}_{light}X\right)_{XB}}$$

Fractionations are typically very small, on the order of parts per thousand or parts per ten thousand, so it is common to see expressions like 1000•ln(α) or 1000•(α–1) that magnify the difference between α and 1. α =1.001(1000•[α–1] = 1) is equivalent to a 1 per mil (‰) fractionation. Readers of the primary theoretical literature on stable isotope fractionations will frequently encounter results tabulated in terms of β-factors or equilibrium constants. For present purposes, we can think of β_{XR} as simply a theoretical fractionation calculated between some substance *XR* containing the element *X*, and dissociated, non-interacting atoms of *X*. In the present review the synonymous term α_{XR-X} is used. This type of fractionation factor is a convenient way to tabulate theoretical fractionations relative to a common exchange partner (dissociated, isolated atoms), and can easily be converted into fractionation factors for any exchange reaction:

$$\alpha_{XA\text{-}XB} = \frac{\alpha_{XA\text{-}X}}{\alpha_{XB\text{-}X}} = \frac{\beta_{XA}}{\beta_{XB}}$$

Conversions between equilibrium constants and fractionation factors are more complicated, as it is often necessary to account for molecular stoichiometry and symmetry. For a generic balanced isotopic exchange reaction,

$$n\bullet{}^{light}X_mA + m\bullet{}^{heavy}X_nB \leftrightarrow n\bullet{}^{heavy}X_mA + m\bullet{}^{light}X_nB$$

where m and n are stoichiometric coefficients, the equilibrium constant K_{eq} is related to the fractionation factor $\alpha_{XA\text{-}XB}$ by the expression,

$$\alpha_{XA\text{-}XB} = \left(\frac{S_{{}^{heavy}X_mA}}{S_{{}^{light}X_mA}}\right)^{\frac{1}{n}} \left(\frac{S_{{}^{light}X_nB}}{S_{{}^{heavy}X_nB}}\right)^{\frac{1}{m}} \left(K_{eq}\right)^{\frac{1}{mn}}$$

where $S_{{}^{heavy}X_mA}$, $S_{{}^{light}X_mA}$, $S_{{}^{light}X_nB}$, and $S_{{}^{heavy}X_nB}$ are the molecular symmetry numbers for each reactant and product molecule. Unlike equilibrium constants, isotopic fractionation factors for the elements of interest here can be determined accurately without worrying about symmetry numbers, and are simply related to isotopic ratios, and are therefore better suited to an introductory discussion. To avoid confusion, the examples discussed below are deliberately chosen so that calculated fractionation factors and equilibrium constants are equivalent.

EQUILIBRIUM FRACTIONATION THEORY

Fractionation in molecules

Equilibrium stable isotope fractionation is a quantum-mechanical phenomenon, driven mainly by differences in the vibrational energies of molecules and crystals containing atoms of differing masses (Urey 1947). In fact, a list of vibrational frequencies for two isotopic forms of each substance of interest—along with a few fundamental constants—is sufficient to calculate an equilibrium isotope fractionation with reasonable accuracy. A succinct derivation of Urey's formulation follows. This theory has been reviewed many times in the geochemical

literature, (e.g., Urey 1947; O'Neil 1986; Criss 1991, 1999; Chacko et al. 2001), and it is whole-heartedly suggested that an interested reader look at several versions—digestion of thermodynamic concepts often requires more than one attempt. A thorough discussion of partition functions can be found in any statistical mechanics textbook, (e.g., Mayer and Mayer 1940). In the present introduction, we will focus on one simple isotope exchange reaction in the Cl-isotope system.

Let us consider a simple isotope exchange reaction, where ^{35}Cl and ^{37}Cl swap between the diatomic gas ClO and an isolated Cl atom:

$$^{35}Cl^{16}O + {}^{37}Cl \leftrightarrow {}^{37}Cl^{16}O + {}^{35}Cl$$

This type of exchange (with an isolated atom as one exchange partner) is the basis of Urey's treatment, because it facilitates a particularly convenient set of simplifications. The equilibrium constant for this exchange reaction,

$$K_{eq} = \frac{\left({}^{37}Cl^{16}O\right)\left({}^{35}Cl\right)}{\left({}^{35}Cl^{16}O\right)\left({}^{37}Cl\right)}$$

is equivalent to the equilibrium isotopic fractionation factor "α":

$$\alpha_{ClO\text{-}Cl} = \frac{\left({}^{37}Cl/{}^{35}Cl\right)_{ClO}}{\left({}^{37}Cl/{}^{35}Cl\right)_{Cl}} = \frac{\left({}^{37}Cl^{16}O\right)/\left({}^{35}Cl^{16}O\right)}{\left({}^{37}Cl\right)/\left({}^{35}Cl\right)}$$

This equivalence is not universal—molecules with more than one atom of the element being exchanged may require a somewhat more complicated treatment. However, these complications have a negligible effect on the final result, so we have chosen an example that simplifies the mathematics as much as possible. As with any chemical reaction, the equilibrium constant can be determined from the free energies of the reactants and products, using the familiar expressions,

$$\Delta G^0_{Rxn} = -RT\ln\left(K_{eq}\right)$$

$$K_{eq} = \exp\left(\frac{-\Delta G^0_{Rxn}}{RT}\right)$$

where ΔG^0_{Rxn} is the Gibbs free energy of the reaction, R is the molar gas constant (approximately 8.314 J•mol/K), T is the absolute temperature, and K_{eq} is the equilibrium constant. Isotope-exchange reactions are particularly simple because the bond structure and thus the potential energy of each molecule are essentially unchanged by isotopic substitution. For this reason, calculations only need to consider the contributions of dynamic energy associated with atomic motion. Isotopic exchange reactions also do not, in general, involve significant pressure-volume work because the number of molecules on both sides of the reaction is the same, and because isotope substitution has a negligible effect on the molar volumes of condensed and non-ideal phases under normal conditions (see Gillet et al. 1996; Driesner and Seward 2000; Horita et al. 2002 for more thorough discussions of the influence of pressure on isotope fractionations of light elements). Under these conditions, the Gibbs free energy of the exchange reaction ΔG^0_{Rxn} is equivalent to the Helmholtz free energy (ΔF_{Rxn})

$$G = F + PV \quad \text{and} \quad \Delta G \approx \Delta F$$

So that the basic energetic expression to be evaluated is:

$$K_{\mathrm{eq}} = \exp\left(\frac{-\Delta F_{\mathrm{Motion}}}{\mathrm{R}T}\right)$$

The energy associated with atomic motion is quantized into discrete levels. These motions can be divided into translations, rotations, and vibrations (Fig. 1). An isolated atom like Cl only has translational degrees of freedom. In a molecule there are three translational degrees of freedom, corresponding to motion of the molecule's center of mass in three dimensional space. Most molecules have three rotational degrees of freedom as well, corresponding to the three orthogonal moments of inertia, but linear molecules (including ClO) have only two rotational degrees of freedom. Because the instantaneous motion of each atom in a molecule can be described with three parameters, corresponding to velocities in each of the Cartesian directions, there are three degrees of freedom of motion for each atom. So a molecule with N atoms must have a total of $3N - 3 - 3$ vibrational degrees of freedom (or $3N - 3 - 2$ for linear molecules). Only vibrational quanta are sufficiently large relative to the ambient thermal energy (~$1.5\times\mathrm{R}T/\mathrm{N}_0$; N_0 = Avogadro's number, 6.022×10^{23}) to drive chemical reactions at normal temperatures ($T \geq 100$ K) (Fig. 2). In the simple case of a harmonic vibration, the energy levels are evenly spaced, with a half-quantum of energy present even in the lowest state,

$$E(\mathrm{vib})_i = (n_i + ½)\mathrm{h}\nu_i \quad (1)$$

where n_i (= 0, 1, 2, …) is the quantum number for the i^{th} vibrational degree of freedom, h is Planck's constant (6.626×10^{-34} J•sec), and ν_i is the oscillation frequency of the vibration. The half-quantum of vibrational energy present when $n_i = 0$ is called the zero-point energy. The frequency of a vibration is determined by the masses of atoms that are in motion and the forces that oppose motion, and is therefore sensitive to isotopic substitution. For a diatomic molecule like ClO (with 1 vibration), the frequency can be expressed simply as:

$$\nu = \frac{1}{2\pi}\sqrt{\frac{\mathrm{k_s}}{\mu}} = \frac{1}{2\pi}\sqrt{\mathrm{k_s}\left(\frac{1}{m_{\mathrm{Cl}}} + \frac{1}{m_{\mathrm{O}}}\right)}$$

where $\mathrm{k_s}$ is the effective spring constant of the Cl-O bond and μ is the reduced mass of ClO. Substituting heavy ^{37}Cl for the more common ^{35}Cl isotope increases the reduced mass of the molecule while leaving the spring constant unchanged, thus lowering the vibrational frequency from 853.72 cm^{-1} (Burkholder et al. 1987) to 846.45 cm^{-1} and the zero-point energy from 5,105 J/mole to 5,062 J/mole (cm^{-1} is a spectroscopic unit for frequency called a wavenumber, 1 $\mathrm{cm}^{-1} = 2.9979\times10^{10}$ sec^{-1}). Vibrational frequencies typically range from ~100 cm^{-1} all the way up to 4000 cm^{-1}, corresponding to effective force constants on the order of 50–2000 Newtons/m. One could construct a crude quantitative model of stable isotope fractionations by simply adding up the zero-point energies of the molecules on the right side of the exchange equation, and subtracting the zero-point energies of the left side:

$$\Delta F_{\mathrm{Motion}} \approx \sum \frac{1}{2}\mathrm{h}\nu_{\mathrm{Products}} - \sum \frac{1}{2}\mathrm{h}\nu_{\mathrm{Reactants}} \quad (2)$$

which would correctly predict higher ^{37}Cl/^{35}Cl in ClO equilibrated with atomic Cl (Schauble et al. 2003). This comparison illustrates the basic principle that substances with large zero-point energy shifts on isotopic substitution tend to be enriched in heavy isotopes. Of course, molecules are not always in their ground vibrational states, and it is necessary to include terms to account for the energies of those excited molecules, but it is still generally true that zero-point energy shifts control equilibrium fractionations. The total energy of motion of a system of molecules is determined by means of partition functions. A partition function can be thought

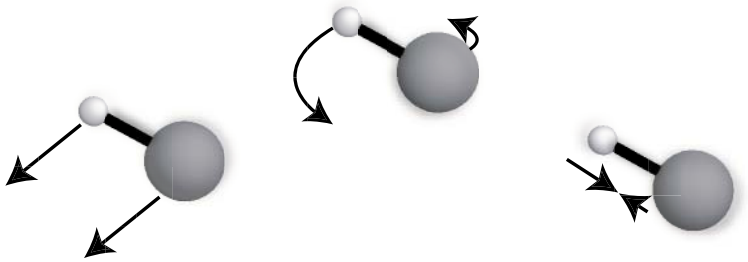

Figure 1. Translation, rotation, and vibration of a diatomic molecule. Every molecule has three translational degrees of freedom corresponding to motion of the center of mass of the molecule in the three Cartesian directions (left side). Diatomic and linear molecules also have two rotational degrees of freedom, about rotational axes perpendicular to the bond (center). Non-linear molecules have three rotational degrees of freedom. Vibrations involve no net momentum or angular momentum, instead corresponding to distortions of the internal structure of the molecule (right side). Diatomic molecules have one vibration, polyatomic linear molecules have 3*N*-5 vibrations, and nonlinear molecules have 3*N*-6 vibrations. Equilibrium stable isotope fractionations are driven mainly by the effects of isotopic substitution on vibrational frequencies.

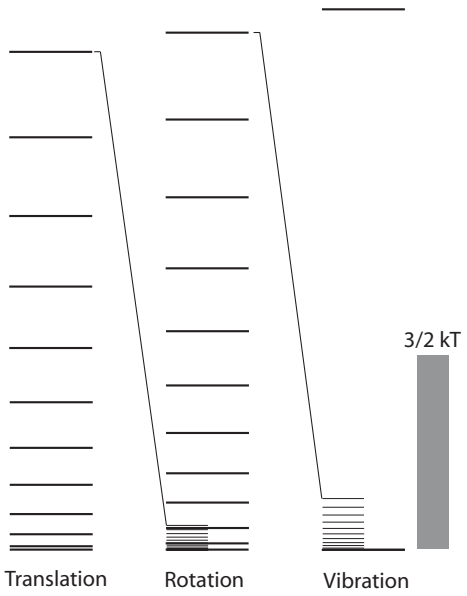

Figure 2. Relative sizes of translational (left), rotational (center), and vibrational (right) energy quanta for a typical diatomic molecule (ClO). The quantum energies of allowed states of motion are calculated using constants tabulated by Burkholder (1987). Presented at the same scale (lower right), rotational quanta are so small that low-lying rotational states are as closely spaced as the thickness of a line. Likewise, the lowest energy translational quanta (assuming a confining volume of 10^{-24} liters) are too small to see on the same scale as rotational energy levels (lower center). The classical thermal energy (3/2 k*T*) of a particle at 298 K is shown as a gray bar at the same scale as the vibrational energy levels. Because the spacing between rotational and translational energy levels is so much smaller than the ambient thermal energy, it is usually not necessary to include a full quantum-mechanical treatment of these types of motion when calculating equilibrium stable isotope fractionation factors. Rotational and translational quanta become even smaller for larger, more massive molecules.

of as a sum, over all of the energy states of a molecule, of the probabilities that the molecule will occupy a particular state. For instance, the vibrational partition function, Q, of a molecule is defined as a sum over all of its vibrational energies E_n,

$$Q = \sum\nolimits_n \exp\left(-E_n / \mathrm{k}T\right)$$

where k is Boltzmann's constant (1.381×10^{-23} J/K or 0.6951 cm^{-1}/K). Partition functions are closely related to the Helmholtz free energy,

$$F = -\mathrm{R}T\ln(Q)$$

For harmonic vibrations, we can insert Equation (1) above,

$$\begin{aligned} Q_{\mathrm{Vib}} &= \sum\nolimits_n \exp\left(-E_n/\mathrm{k}T\right) \\ &= \sum\nolimits_i \sum\nolimits_n \exp\left[-\left(n_i + \frac{1}{2}\right)\mathrm{h}\nu_i \Big/ \mathrm{k}T\right] \end{aligned}$$

This rather awkward expression can be simplified by recognizing the presence of a geometric series:

$$\begin{aligned} &= \sum\nolimits_i \exp\left[-\left(\frac{1}{2}\right)\mathrm{h}\nu_i \Big/ \mathrm{k}T\right] \times \left(\sum\nolimits_{\mathrm{n}} \exp\left[-\left(n_i\right)\mathrm{h}\nu_i / \mathrm{k}T\right]\right) \\ &= \sum\nolimits_i \exp\left[-\frac{\mathrm{h}\nu_i}{2\mathrm{k}T}\right] \times \frac{1}{1-\exp\left[-\mathrm{h}\nu_i/\mathrm{k}T\right]} \end{aligned}$$

leaving a finite sum over the harmonic vibrational frequencies of the molecule.

Energy quanta associated with molecular rotation and translation are so small that they can be treated approximately without an explicit sum over the quantum energies.

$$Q_{\mathrm{Rot}} = \frac{8\pi^2 I \mathrm{k}T}{\mathrm{h}^2} \qquad Q_{\mathrm{Trans}} = V\left(\frac{2\pi m_{\mathrm{molecule}}\mathrm{k}T}{\mathrm{h}^2}\right)^{3/2}$$

where I is the moment of inertia of the molecule (which can be determined from the molecular structure), m_{molecule} is its mass, and V is the volume of the system. While these expressions look complicated, bear in mind that they will almost completely cancel out by the time we're finished. The translational and rotational free energies, added to the vibrational energy, give the total energy of atomic motion,

$$\begin{aligned} F_{\mathrm{Motion}} &= -\mathrm{R}T\left[\ln\left(Q_{\mathrm{Trans}}\right) + \ln\left(Q_{\mathrm{Rot}}\right) + \ln\left(Q_{\mathrm{Vib}}\right)\right] \\ &= -\mathrm{R}T\ln\left(Q_{\mathrm{Trans}} \times Q_{\mathrm{Rot}} \times Q_{\mathrm{Vib}}\right) \end{aligned}$$

and thus the equilibrium constant for the exchange reaction,

$$\begin{aligned} K_{\mathrm{eq}} &= \exp\left(\frac{-\Delta F_{\mathrm{Motion}}}{\mathrm{R}T}\right) = \exp\left(\frac{-\left[F_{\mathrm{Motion}}\{\mathrm{Products}\} - F_{\mathrm{Motion}}\{\mathrm{Reactants}\}\right]}{\mathrm{R}T}\right) \\ &= \exp\left(\sum\nolimits_{\mathrm{Products}} \ln\left[Q_{\mathrm{Trans}} \times Q_{\mathrm{Rot}} \times Q_{\mathrm{Vib}}\right] - \sum\nolimits_{\mathrm{Reactants}} \ln\left[Q_{\mathrm{Trans}} \times Q_{\mathrm{Rot}} \times Q_{\mathrm{Vib}}\right]\right) \\ &= \frac{\prod_{\mathrm{Products}}\left(Q_{\mathrm{Trans}} \times Q_{\mathrm{Rot}} \times Q_{\mathrm{Vib}}\right)}{\prod_{\mathrm{Reactants}}\left(Q_{\mathrm{Trans}} \times Q_{\mathrm{Rot}} \times Q_{\mathrm{Vib}}\right)} \end{aligned}$$

For our simple exchange equation, this expression becomes

$$\alpha_{\mathrm{ClO\text{-}Cl}} = K_{\mathrm{eq}} = \frac{Q_{\mathrm{Trans}}(^{35}\mathrm{Cl})}{Q_{\mathrm{Trans}}(^{37}\mathrm{Cl})} \times \frac{Q_{\mathrm{Trans}} \times Q_{\mathrm{Rot}} \times Q_{\mathrm{Vib}}(^{37}\mathrm{Cl}^{16}\mathrm{O})}{Q_{\mathrm{Trans}} \times Q_{\mathrm{Rot}} \times Q_{\mathrm{Vib}}(^{35}\mathrm{Cl}^{16}\mathrm{O})}$$

$$= \left(\frac{m_{^{35}\mathrm{Cl}}}{m_{^{37}\mathrm{Cl}}}\right)^{3/2} \times \left(\frac{m_{^{37}\mathrm{Cl}^{16}\mathrm{O}}}{m_{^{35}\mathrm{Cl}^{16}\mathrm{O}}}\right)^{3/2} \times \frac{I_{^{37}\mathrm{Cl}^{16}\mathrm{O}}}{I_{^{35}\mathrm{Cl}^{16}\mathrm{O}}} \times \left(\frac{\exp\left[-\frac{\mathrm{h}\nu_{^{37}\mathrm{Cl}^{16}\mathrm{O}}}{2\mathrm{k}T}\right]}{1-\exp\left[-\frac{\mathrm{h}\nu_{^{37}\mathrm{Cl}^{16}\mathrm{O}}}{\mathrm{k}T}\right]} \right) \times \left(\frac{1-\exp\left[-\frac{\mathrm{h}\nu_{^{35}\mathrm{Cl}^{16}\mathrm{O}}}{\mathrm{k}T}\right]}{\exp\left[-\frac{\mathrm{h}\nu_{^{35}\mathrm{Cl}^{16}\mathrm{O}}}{2\mathrm{k}T}\right]} \right)$$

after plugging in the expressions for the different partition functions and simplifying.

The last step in Urey's derivation is the application of the Redlich-Teller product rule (e.g., Angus et al. 1936; Wilson et al. 1955), which relates the vibrational frequencies, moments of inertia, and molecular masses of isotopically substituted molecules. For ClO,

$$\left(\frac{m_{^{35}\mathrm{Cl}}}{m_{^{37}\mathrm{Cl}}}\right)^{3/2} = \left(\frac{m_{^{35}\mathrm{Cl}^{16}\mathrm{O}}}{m_{^{37}\mathrm{Cl}^{16}\mathrm{O}}}\right)^{3/2} \times \frac{I_{^{35}\mathrm{Cl}^{16}\mathrm{O}}}{I_{^{37}\mathrm{Cl}^{16}\mathrm{O}}} \times \frac{\nu_{^{37}\mathrm{Cl}^{16}\mathrm{O}}}{\nu_{^{35}\mathrm{Cl}^{16}\mathrm{O}}} \qquad \text{(Redlich-Teller)}$$

Inserting this into the partition function ratio yields the final result:

$$\alpha_{\mathrm{ClO\text{-}Cl}} = \frac{\nu_{^{37}\mathrm{Cl}^{16}\mathrm{O}}}{\nu_{^{35}\mathrm{Cl}^{16}\mathrm{O}}} \times \left(\frac{\exp\left[-\frac{\mathrm{h}\nu_{^{37}\mathrm{Cl}^{16}\mathrm{O}}}{2\mathrm{k}T}\right]}{1-\exp\left[-\frac{\mathrm{h}\nu_{^{37}\mathrm{Cl}^{16}\mathrm{O}}}{\mathrm{k}T}\right]} \right) \times \left(\frac{1-\exp\left[-\frac{\mathrm{h}\nu_{^{35}\mathrm{Cl}^{16}\mathrm{O}}}{\mathrm{k}T}\right]}{\exp\left[-\frac{\mathrm{h}\nu_{^{35}\mathrm{Cl}^{16}\mathrm{O}}}{2\mathrm{k}T}\right]} \right)$$

$$= 1.0096 \ @ \ 298K$$

A more general expression for the equilibrium fractionation of isotopes ${}^{light}X$ and ${}^{heavy}X$, applicable to all diatomic and larger molecules is:

$$\alpha_{XR\text{-}X} = \left[\prod_i \frac{\nu_{^{heavy}XR}}{\nu_{^{light}XR}} \times \left(\frac{\exp\left[-\frac{\mathrm{h}\nu_{^{heavy}XR}}{2\mathrm{k}T}\right]}{1-\exp\left[-\frac{\mathrm{h}\nu_{^{heavy}XR}}{\mathrm{k}T}\right]} \right) \times \left(\frac{1-\exp\left[-\frac{\mathrm{h}\nu_{^{light}XR}}{\mathrm{k}T}\right]}{\exp\left[-\frac{\mathrm{h}\nu_{^{light}XR}}{2\mathrm{k}T}\right]} \right) \right]^{1/\mathrm{n}} \qquad (3)$$

where XR, containing n atoms of element X and N total atoms, is the molecule of interest, ${}^{light}XR$ is XR containing only the light isotope ${}^{light}X$, ${}^{heavy}XR$ contains only ${}^{heavy}X$, and the product is over all $3N - 6$ or $3N - 5$ vibrational frequencies of XR. The exponent 1/n is a normalizing factor that accounts for multiple substitutions in molecules containing more than one atom of X. Note that α is only affected by vibrational frequencies that change upon isotopic substitution, the vibrational partition function ratio for other frequencies will cancel to unity. The reader is cautioned that α is generally not equivalent to K_{eq} if $\mathrm{n} > 1$. The theoretical expression for α is often called the reduced partition function ratio because of the cancellations of the rotational and translational energy terms. In addition to its role in simplifying the final expression for α, the Redlich-Teller product rule is an important criterion for evaluating the accuracy of a set of

vibrational frequencies for a molecule—substantial deviations from the product rule indicate that measurement errors, unusually large anharmonic effects, and/or typographical mistakes are likely to degrade the accuracy of a calculated fractionation.

Equilibrium isotopic fractionations calculated using Urey's approach assume harmonic vibrations and rigid-body rotation, and use a simplified treatment of rotational energies. They also average intra-molecular isotopic fractionations over the entire molecule. These assumptions greatly simplify calculations, because the only inputs needed are vibrational frequencies for isotopically light and heavy molecules. The assumptions are generally reasonable over the typical temperature range of interest to geochemists (~1000 K > T > 100 K) for isotope systems other than H, C, N, O, and S. Fractionations at higher temperatures are usually so small that the progressive breakdown of the first two assumptions has little practical significance. Fractionations calculated at cryogenic temperatures (<100 K) should include a full quantum-mechanical treatment of molecular rotation. Vibrational anharmonicity and vibrational-rotational interactions can be included in theoretical calculations, but are usually practical only for molecules that have been the subjects of extensive, highly precise spectroscopic studies (Richet et al. 1977). For many substances (including essentially all condensed phases), uncertainties associated with measured and/or modeled vibrational frequencies are likely to be larger than any anharmonic and vibrational-rotational effects, so in practice there is probably little reason to use the more complex models.

Fractionation in crystalline materials and solutions

Gas-phase molecules play a relatively minor role in the geochemistry of most elements other than H, C, N, O, and S, so it is important to consider extensions of the theory outlined in the preceding section to other types of materials, particularly aqueous solutions and crystals. In general, the same energetic concepts (especially zero-point energy) apply, but it is necessary to make additional assumptions to deal with the complexities and uncertainties that arise in dealing with condensed phases.

For solutions or crystals, it is apparent that the simple picture of an isolated molecule with a completely known, finite number of vibrational frequencies is impractical. A microscopic crystal 1 μm across might contain 10^{11} or more atoms, implying 3×10^{11} or more vibrational modes! Similarly, an atom, ion or molecule dissolved in water will interact with water molecules and other dissolved species in a continuously changing arrangement of hydrogen bonds and ion pairs. However, these complications can be treated in a simplified way or even ignored while still allowing calculations that are accurate enough to be useful.

When dealing with dissolved molecules and molecular ions that remain more or less intact in solution (e.g., $[ClO_4]^-$, $B(OH)_3$ and CCl_4), or with aqueous complexes where intra-complex bonds are probably much stronger than interactions with the bulk solvent (e.g., $[Cr(H_2O)_6]^{3+}$, $[FeCl_4]^-$, and Mg^{2+} in chlorophyll), a reasonable if crude approximation is to treat each as though it actually *were* a gas-phase molecule. The only inputs needed in such a model are the intra-molecular vibrational frequencies (preferably measured in solution). This approach has been followed in numerous studies (Urey 1947; Kotaka and Kakihana 1977; Schauble et al. 2001), and has proven to be reliable under favorable conditions, at least as a semi-quantitative guide to real fractionations. This gas-in-solution approximation probably works best for molecules and complexes that are substantially heavier than a single atom of the element of interest (i.e., selenium in $[SeO_4]^{2-}$ rather than H_2Se), when those atoms are isolated from direct contact with the solvent (chlorine in $[ClO_4]^-$ rather than $[ClO]^-$), when solvent interactions are weak, and when intra-molecular bonds are strong. It is to be expected, however, that such calculations will not be as accurate as would be possible for a true gas—for instance, most gases exhibit measurable isotopic fractionations between the vapor phase and solution that is only crudely accounted for in this approximation. It is likely that theoretical

calculations could be improved by taking the solvent into account more explicitly, but in practice the spectroscopic data are not known, so it is necessary to create a vibrational model of the solution. These models will be introduced in a later section.

Crystals lack some of the dynamic complexity of solutions, but are still a challenging subject for theoretical modeling. Long-range order and forces in crystals cause their spectrum of vibrational frequencies to appear more like a continuum than a series of discrete modes. Reduced partition function ratios for a continuous vibrational spectrum can be calculated using an integral, rather than the finite product used in Equation (3) (Kieffer 1982),

$$\alpha_{XR(\text{crystal})-X} = \left(\frac{m_{light\ X}}{m_{heavy\ X}}\right)^{3/2} \times \exp\left(\frac{1}{n}\frac{\int_0^{\nu_{max}} \ln\left(\frac{\exp\left[-\frac{h\omega}{2kT}\right]}{1-\exp\left[-\frac{h\omega}{kT}\right]}\right) g_{heavy\ X}(\omega)\,d\omega}{\int_0^{\nu_{max}} \ln\left(\frac{\exp\left[-\frac{h\omega}{2kT}\right]}{1-\exp\left[-\frac{h\omega}{kT}\right]}\right) g_{light\ X}(\omega)\,d\omega}\right)$$

where $g_{heavy_X}(\omega)$ and $g_{light_X}(\omega)$ are the vibrational density of states of isotopically heavy and light forms of the crystal, respectively, n is the number of atoms of X in each unit cell of XR(crystal), and the integrals extend to the highest vibrational frequencies of the crystal. $g(\omega)$ is proportional to the number of vibrational degrees of freedom in the infinitesimal frequency interval $\omega \rightarrow \omega + \delta\omega$ for a molecule $g(\omega)$ takes the form of a series of delta functions centered at the discrete vibrational frequencies. Alternatively, the continuous vibrational spectrum can be approximated using a representative set of discrete frequencies—even a relatively small number of frequencies (~10 to 20 for a small unit cell) can be sufficient (Elcombe and Pryor 1970). A small subset of the vibrational frequencies in the continuum—those with a phase wavelength much longer than a unit cell—can be measured using conventional infrared and Raman spectroscopy. Unfortunately, these vibrational modes are particularly unrepresentative of the total vibrational spectrum, but they may be sufficient for crystals with ~6 or more atoms per unit cell. In crystals the rotational and translational terms in the Redlich-Teller product rule disappear, yielding the high-T product rule of Kieffer (1982). Crystal vibrational frequencies must obey the high-T product rule, or calculated fractionations will fail to converge to $\alpha = 1$ at high temperatures (see Chacko et al. 1991 and Bottinga 1968 for an example of the use of the high-T product rule in evaluating calculated C and O isotope fractionations in calcite).

For crystals with molecule-like constituents, like the BO_3^{3-} and BO_4^{5-} groups in some borates, semi-quantitative models of the molecular component as a gas-phase entity have been proposed (Oi et al. 1989). This is conceptually similar to the approximation made for species in solution, although in practice most studies of crystals consider additional frequencies that reflect inter-molecular vibrations. The spectroscopic data on these vibrations (which typically have lower frequencies than the intra-molecular vibrations) are often available, at least approximately, from infrared and Raman spectroscopy and elastic properties. This type of hybrid molecule-in-crystal model has been applied to many minerals in theoretical studies of carbon and oxygen isotope fractionation, the most noteworthy being studies of calcite (Bottinga 1968; Chacko et al. 1991) and silicates (Kieffer 1982). Because spectroscopic data are always incomplete (especially for substances substituted with rare isotopes), some amount of vibrational modeling is necessary.

The chemistry of stable isotope fractionation

Bigeleisen and Mayer (1947) simplified the reduced partition function by observing that vibrational frequency shifts caused by isotope substitution are relatively small (except when deuterium is substituted for normal hydrogen). When the dimensionless quantity $h\nu/kT$ is of the order 5 or less (corresponding to a typical 1000 cm^{-1} vibration at 288 K)—a condition applicable to most geochemical situations,

$$\alpha_{XR-X} \approx 1 + \frac{h^2 \sum_i \nu_{light\ XR}{}^2 - \nu_{heavy\ XR}{}^2}{24nk^2T^2} \tag{4}$$

This relation correctly predicts that most equilibrium stable isotope fractionations are inversely proportional to the square of absolute temperature, and is the basis of equilibrium fractionation rule (1). A detailed derivation of the Bigeleisen and Mayer model has been presented in an earlier review (Criss 1991).

Using a sum-of-squares rule from theoretical vibrational spectroscopy, Bigeleisen and Mayer (1947) then showed that, under the conditions relevant to Equation (4),

$$\sum_i \nu_{light\ XR}{}^2 - \nu_{heavy\ XR}{}^2 \approx \frac{m_{heavy\ X} - m_{light\ X}}{m_{light\ X} m_{heavy\ X}} \frac{1}{4\pi^2} A \tag{5}$$

where A is the sum of all force constants acting on an atom of X, averaged over the molecule. This relation is the origin of rules (2) and (3).

Note that when $h\nu/kT$ is of order 10 or more, either at low temperatures or for molecules with high-frequency vibrations, essentially all molecules are in the vibrational ground state. Under these circumstances the free energy of the exchange reaction is only sparingly sensitive to temperature, and fractionations more closely approximate Arrhenius-like $1/T$ behavior. Bonds between a heavier atom and hydrogen usually lead to high-frequency bond-stretching vibrations that are somewhat sensitive to isotope substitution of the heavy atom. For this reason, the Bigeleisen and Mayer (1947) analysis tends to break down in molecules where the element of interest in bonded directly to hydrogen. Under these circumstances, heavy isotopes will be less concentrated in the substance than the force-constant analysis might suggest, leading to rule (4) and a special exception to rule (1). The chlorine isotope system (^{37}Cl-^{35}Cl) provides a good example of this behavior (Fig. 3), with $\alpha_{HCl\text{-}Cl}$ displaying marked concave-down curvature when plotted against $1/T^2$. This phenomenon also contributes to the high temperature-sensitivity of oxygen isotope fractionations between anhydrous minerals (lacking O-H bonds) and water.

Other causes of equilibrium isotopic fractionation

A handful of non-vibrational mechanisms responsible for equilibrium fractionations have been proposed, including effects of nuclear spin or shape on electronic energies (Bigeleisen 1998). These non-vibrational phenomena are distinguishable from conventional fractionations, at least in principle, because they are not expected to be mass dependent, and geochemists should be careful not to automatically dismiss data that do not conform to mass-dependent behavior. These effects may be restricted to very heavy elements (i.e., uranium). Claims of non-vibrational fractionations (Fujii et al. 2002) in lighter elements have not been substantiated using modern analytical techniques, to my knowledge, and it is not yet clear how important these unconventional mechanisms are in natural systems. For this reason, the present review focuses on the well established vibrational model (Bigeleisen and Mayer 1947; Urey 1947).

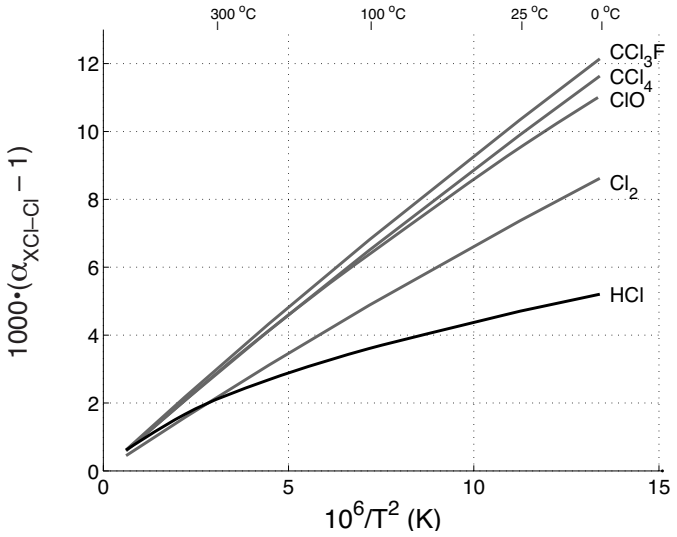

Figure 3. Theoretical ^{37}Cl-^{35}Cl fractionation factors for Cl-bearing molecules, adapted from (Schauble et al. 2003). Typically, stable isotope fractionation factors are nearly linear when plotted against $1/T^2$, as can be seen for CCl_3F, CCl_4, ClO, and Cl_2 in this example (gray lines). This behavior is predicted by eq. 4 (Bigeleisen and Mayer 1947). However, molecules in which the atom of interest is bonded directly to hydrogen (such as HCl, dark line) often show significant concave-down curvature on the same axes, because $h\nu_{HCl}/kT$ is too high ($\approx$ 14.4 at room temperature) for the Bigeleisen and Mayer (1947) simplification to apply. At room temperature, HCl is predicted to have lower $^{37}Cl/^{35}Cl$ than Cl_2, even though the spring constant for the H-Cl bond is considerably higher (530 N/m) than the Cl-Cl spring constant (330 N/m). This anomalous affinity of H-X compounds for light isotopes is the origin of rule 4 and the special exception to rule 1.

APPLYING STABLE ISOTOPE FRACTIONATION THEORY

Estimating unknown vibrational frequencies

The theory of stable isotope fractionation described by Urey (1947) and Bigeleisen and Mayer (1947) has been repeatedly confirmed by comparison of theoretical predictions with laboratory experiments and measurements on carefully chosen suites of natural samples. However, there are a number of hurdles that can make it difficult to apply the theory to novel substances and isotopic systems. Paramount among these difficulties is the limited availability of highly accurate and complete vibrational frequencies in the spectroscopic literature, a problem that is particularly acute for materials containing rare isotopes and for most condensed phases. To get a sense of the difficulty, let us consider a 1 cm^{-1} error in the isotopic shift of one 500 cm^{-1} vibrational frequency. The error is chosen arbitrarily here, but is reasonable for condensed-phase materials and all but the smallest molecules. Using Equation (4), this propagates to a 1.0 per mil error in α at 298 K. This error is much larger than the typical uncertainty of a modern mass-spectrometric measurement, and will tend to increase as the size of a molecule (and thus the number of vibrations) increases. Accurate and complete spectroscopic data *are* available for many small gas-phase molecules that are likely to be of interest in geochemical studies, both in the primary research literature and in spectroscopy reviews and databases. For more complex materials, however, it is usually necessary to approximate unknown vibrational frequencies using some type of model. A number of excellent introductory vibrational analysis texts have been published. The present introduction

borrows heavily from two recommended texts—Wilson et al. (1955) and Nakamoto (1997)—the former text contains detailed derivations of basic principles and mathematical techniques, while Nakamoto (1997) provides a concise introduction along with copious data tables, appendices, and references to relevant primary literature.

The simplest type of vibrational model consists of one or more simple rules used to estimate frequencies of isotopically substituted substances from known vibrational frequencies for the common isotopic form. An example is the model developed by Kieffer (1982) to calculate vibrational frequencies in ^{18}O-bearing silicates. This approach is most likely to be effective in systems where spectroscopic data on the dominant isotopic form of a set of related substances is known—as is the case with natural ^{16}O-dominated silicate minerals—and when data bearing on isotopic substitution effects in similar materials is also known. For instance, Kieffer (1982) used results from ^{18}O-substituted silica glass to estimate frequencies in ^{18}O-quartz. Furthermore, the technique is mostly limited to instances where a more-or-less discrete molecule (such as SiO_4^{4-}) with distinctive vibrational properties can be recognized. In fact, Kieffer's results for other silicates were extrapolated from a force-field model of the SiO_4^{4-} "molecule." In heavy element stable isotope systems, the rules-based approach is unlikely to be widely applicable because these fractionations are much more dependent on the low-frequency vibrations that are most sensitive to heavy-element isotopic substitution. These frequencies are more difficult to assign to a particular type of atomic motion, and generally have not been measured with as much accuracy.

A potentially much more adaptable technique is force-field vibrational modeling. In this method, the effective force constants related to distortions of a molecule (such as bond stretching) are used to estimate unknown vibrational frequencies. The great advantage of this approach is that it can be applied to any material, provided a suitable set of force constants is known. For small molecules and complexes, approximate force constants can often be determined using known (if incomplete) vibrational spectra. These empirical force-field models, in effect, represent a more sophisticated way of extrapolating known frequencies than the rule-based method. A simple type of empirical molecular force field, the modified Urey-Bradley force field (MUBFF), is introduced below.

Another way to determine force constants is through *ab initio* quantum mechanical calculations. In this approach, the electronic structure of a molecule is determined through an approximate solution of the Schrödinger equation, and force constants are determined from the 2nd derivatives of the electronic energy of the molecule with respect to atomic displacements. Although quantum mechanical calculations are computationally intensive, advances in processor speed and memory size and performance have made relatively accurate calculations feasible on many desktop computers using well-documented, freely available software (i.e., GAMESS; Schmidt 1993). The independence of *ab initio* force fields from empirical vibrational frequency data means that partial and imprecise spectra can be used to independently verify the accuracy of each force field model. The downside is that it can be tricky to accommodate complicating factors like molecule-solvent interactions (see Anbar et al., in press, for an example calculation that attempts to overcome this difficulty), and to model materials with complex electronic structures. In principle, crystals can also be modeled with both empirical and *ab initio* force fields, although the range of suitable materials is more restricted.

Vibrational force-field modeling

In any force-field model, the molecule to be analyzed is treated as a set of masses connected by springs. Calculating vibrational frequencies for a particular set of coupled masses and springs is essentially a problem of matrix algebra, and the summary presented below is more mathematically intense than preceding sections. The equations may appear

daunting at first, but remember that calculations for real molecules can be largely automated using computers, and greatly simplified by taking advantage of molecular symmetries. The geometry of a molecule may be determined from structural measurements (typically X-ray or neutron diffractometry and/or rotational spectroscopy), or from *ab initio* structural relaxation. Given a set of force-constant parameters, the vibrational spectrum of a molecule can then be determined by solving a set of differential equations,

$$\frac{d}{dt}\frac{\partial KE}{\partial\left(\frac{dq_j}{dt}\right)}+\frac{\partial PE}{\partial q_j}=0$$

where *KE* and *PE* are the potential and kinetic energies of the molecule, respectively, and q_j are small, mass-weighted displacements of each atom from the equilibrium position in each of the three Cartesian directions:

$$q_1=\sqrt{m_1}\Delta x_1,\ q_2=\sqrt{m_1}\Delta y_1,\ q_3=\sqrt{m_1}\Delta z_1,\ q_4=\sqrt{m_2}\Delta x_2,\ etc.$$

If we define a set of mass-weighted Cartesian force constants f_{ij},

$$f_{ij}=f_{ji}=\frac{\partial^2 PE}{\partial q_i \partial q_j}$$

then all vibrational frequencies ν satisfy the secular equation:

$$\begin{vmatrix} f_{11}-4\pi^2\nu^2 & f_{12} & \cdots & f_{1,3N} \\ f_{21} & f_{22}-4\pi^2\nu^2 & \cdots & f_{2,3N} \\ \cdots & \cdots & \cdots & \cdots \\ f_{3N,1} & f_{3N,2} & \cdots & f_{3N,3N}-4\pi^2\nu^2 \end{vmatrix}=0$$

Once a set of force constants is established, isotopic substitution is modeled by simply changing the relevant mass terms while leaving all other parameters unchanged. In *ab initio* models the force constants can all be determined directly by calculating energies and forces acting on atoms in systematically distorted molecules—in some *ab initio* methods it is even possible to calculate force constants analytically in the minimum-energy configuration of the molecule. In empirical force-field calculations, however, the force constants are solved using a limited set of constraints. The most common constraints are known vibrational frequencies. The number of Cartesian force constants increases roughly as the square of the number of atoms, while the number of vibrations increases linearly. Because of this scaling, it is not generally possible to solve for all of the Cartesian force constants of large molecules (i.e., molecules containing more than three atoms) independently unless vibrational frequencies for two or more isotopic forms of the molecule are known.

When constructing a vibrational model it is important to take note of possible simplifying procedures, particularly for complex phases. Many of the substances that are most interesting from the point of view of isotope geochemistry are complex solutions, crystals, large molecules, and amorphous phases that may be impossible to model in detail. Practical application of theoretical techniques often requires compromising detail and a certain amount of accuracy in order to find a tractable path to useful results. Choosing an appropriate compromise is important, as is seeking out corroborating data that can be used to justify a particular simplification. In studying aqueous molecules and complexes, for instance, the common procedure of ignoring solvent effects seems to yield reasonable, if only semi-

quantitative estimates of isotopic fractionations (e.g., Kakihana and Kotaka 1977; Schauble et al. 2001; Johnson et al. 2002). The validity of the simplified treatment can be justified by noticing that vibrational frequencies in many strongly-bonded molecule-like species are not very sensitive to the details of the phase in which they occur. Schauble et al (2001) observed, for instance, that measured vibrational frequencies for many aqueous iron chloride and iron-aquo complexes changed by ~5% or less in solutions of varying chemical composition, and even in crystals held together by weak ionic- or hydrogen-bonding networks.

Empirical force fields

Empirical force field models have long been used to estimate unknown vibrational frequencies in theoretical stable isotope studies (Urey and Greiff 1935; Urey 1947). For small, symmetric molecules and molecule-like aqueous and crystalline species force-field calculations can be easily implemented in typical spreadsheet software or with scientific computation packages. The major difficulty in implementing an empirical force field model is obtaining accurate, well-constrained force constants from known vibrational frequencies – the number of independent force constants to be constrained must be smaller than the number of known frequencies. Numerous schemes have been developed that require a minimal number of force constants, including the valence force field (VFF) (e.g, Wilson et al. 1955), orbital valence force field (OVFF) (Heath and Linnett 1948), and modified Urey-Bradley force field (MUBFF) (Simanouti (Shimanouchi) 1949). These force field methods share more similarities than differences, and we will focus on the MUBFF, which has been applied in numerous theoretical studies (Kotaka and Kakihana 1977; Kotaka et al. 1978; Schauble et al. 2001). The MUBFF accounts for only three types of molecular distortions: bond stretching, bond-angle bending, and repulsion between adjacent, non-bonded atoms (Fig. 4), with the consequence that most of the Cartesian force constants cease to be independent. The choice of force-constant types follows from chemical intuition, as these types of distortion affect the basic structural properties of a molecule. The effectiveness of the MUBFF in calculating frequencies has been reviewed for tetrahedral (XY_4) and octahedral (XY_6) complexes (Basile et al. 1973; Krynauw 1990). More complex force fields, including additional inter-atomic interactions and/or anharmonic potential parameters, can be applied to well-studied molecules, but not in the most common situation where frequencies have only been measured in one isotopic form (or a natural mixture of isotopes that is dominated by one isotope of each element in the molecule).

As is common with empirical force fields, MUBFF calculations are carried out using internal molecular coordinates rather than Cartesian coordinates. Internal coordinates describe the structure of a molecule in terms of bond lengths and angles between bonds. As an example, for a bent tri-atomic molecule *ABC* the three internal coordinates include the lengths of bonds *AB* (r_{AB}) and *BC* (r_{BC}), as well as the angle between them (α_{ABC}). Larger molecules may also

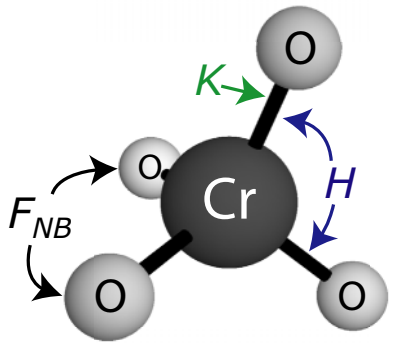

Figure 4. Schematic illustration of force-constant parameters used in Modified Urey-Bradley Force-Field (MUBFF) vibrational modeling (Simanouti (Shimanouchi) 1949). The MUBFF is a simplified empirical force field that has been used to estimate unknown vibrational frequencies of molecules and molecule-like aqueous and crystalline substances. Here, three force constants (*K*, *H*, and F_{NB}) describe distortions of a tetrahedral XY_4 molecule, $[CrO_4]^{2-}$ due to bond stretching (Cr-O), bond-angle bending (∠ O-Cr-O), and repulsion between adjacent non-bonded atoms (O..O). Less symmetric molecules with more than one type of bond or unequal bond angles require more parameters, but they will belong to the same basic types.

have additional types of internal coordinates, such as torsional or dihedral angles. Any small perturbation of these coordinates can be described in terms of a vector R, which for the example molecule *ABC* looks like this:

$$R = \begin{bmatrix} \Delta r_{AB} \\ \Delta r_{BC} \\ \Delta \alpha_{ABC} \end{bmatrix}$$

The potential energy of a molecule can then be described in terms of the internal coordinates, i.e.,

$$2PE = R^t FR$$

where R^t is the transpose of R and F is a matrix of mass-independent internal-coordinate force constants. The kinetic energy can also be written in terms of R, albeit with a few intermediate steps. The matrix describing perturbations of the Cartesian coordinates of each atom (with the center of mass as the origin) is defined,

$$X = \begin{bmatrix} \Delta x_1 \\ \Delta y_1 \\ \Delta z_1 \\ \Delta x_2 \\ \cdots \\ \Delta z_N \end{bmatrix}$$

along with an isotope-sensitive diagonal matrix M^{-1} consisting of the reciprocal masses of each atom repeated three times,

$$M^{-1} = \begin{bmatrix} \frac{1}{m_1} & & & & & \\ & \frac{1}{m_1} & & & 0 & \\ & & \frac{1}{m_1} & & & \\ & & & \ddots & & \\ 0 & & & & \frac{1}{m_N} & \end{bmatrix}$$

Then a third matrix B relating the internal and Cartesian coordinates is determined,

$$R = BX$$

Finally we can write out a kinetic energy matrix G,

$$G = BM^{-1}B^t$$

such that

$$2KE = \frac{dR^t}{dt} G^{-1} \frac{dR}{dt}$$

where G^{-1} is the reciprocal of the special matrix G. Each eigenvalue of the product matrix GF is equal to $4\pi^2\nu^2$, where ν is a vibrational frequency of the molecule. This procedure for calculating vibrational frequencies in terms of internal molecular coordinates is often referred to as the *GF* method.

The eigenvector corresponding to each eigenvalue determines the characteristic motion of

each atom in the vibration. The characteristic atomic motions associated with each frequency (called normal modes) are closely related to the problem of determining how vibrational frequencies change when one isotope of an element is substituted for another. Specifically, isotopic sensitivity scales with the intensity of atomic motion: if an atom remains stationary in a particular normal mode, the frequency of that mode will not be affected by isotopic substitution of that atom; if the atom exhibits high-amplitude motion, the frequency of the mode will be highly sensitive to isotopic substitution.

Of course, before the atomic motions and unknown frequencies can be determined it is necessary to constrain the force constants from known frequencies. From the derivation shown above it is not clear how to distinguish one mode from another—how to determine which calculated frequency corresponds to a known measured frequency. This is done by classifying each normal mode according to its symmetry properties. A detailed introduction to the use of molecular symmetry in vibrational analysis is beyond the scope of the present review, several comprehensive reviews have been published elsewhere (Herzberg 1945; Wilson et al. 1955; Cotton 1971; McMillan and Hess 1988; Nakamoto 1997). Of immediate relevance is the fact that molecular symmetries can be used to block-diagonalize the *G* and *F* matrices, so that eigenvalues can be determined from the products of submatrices corresponding to each irreducible representation of the point group of the molecule. Since the Raman and infrared selection rules that determine whether a particular vibrational mode can be observed are also determined by the irreducible representation of each mode, it is usually possible to match calculated and observed frequencies in small groups if not strictly on a one-to-one basis.

Optimized MUBFF models typically reproduce the input frequencies within ~10% or better. In order to reap the maximum possible benefit from the known frequencies, the model ratio of frequencies for isotopically substituted molecules can be multiplied by the measured frequency to give a normalized isotopic frequency, i.e.,

$$\left(\nu_{rare\ isotope}\right)_{calc.} = \left(\frac{\nu_{rare\ isotope}}{\nu_{major\ isotope}}\right)_{MUBFF} \times \left(\nu_{major\ isotope}\right)_{measured} \tag{6}$$

GF method calculations are simplified by the systematic behavior of the *G* matrix elements (Decius 1948). MUBFF calculations, however, are somewhat complicated by the force constants representing interactions between non-bonded atoms—these can be tedious to express in terms of internal coordinates. Computer programs have been written to partially automate calculations, thereby reducing the necessary effort and minimizing opportunities for errors (e.g., Schachtschneider 1964; Gale and Rohl 2003).

In addition, *G* and *F* matrix elements have been tabulated (see Appendix VII in Nakamoto 1997) for many simple molecular structure types (including bent triatomic, pyramidal and planar tetratomic, tetrahedral and square-planar 5-atom, and octahedral 7-atom molecules) in block-diagonalized form. MUBFF *G* and *F* matrices for tetrahedral XY_4 and octahedral XY_6 molecules are reproduced in Table 1. Tabulated matrices greatly facilitate calculations, and can easily be applied to vibrational modeling of isotopically substituted molecules. Matrix elements change, however, if the symmetry of the substituted molecule is lowered by isotopic substitution, and the tabulated matrices will not work in these circumstances. For instance, $^{12}C^{35}Cl_4$, $^{13}C^{35}Cl_4$, and $^{12}C^{37}Cl_4$ all share full XY_4 tetrahedral symmetry (point group T_d), but $^{12}C^{35}Cl^{37}Cl_3$ and other partially ^{37}Cl-substituted forms do not, and cannot be modeled with the tabulated matrices. The practical significance of this restriction is negligible, however, because one corollary of the rule the mean for isotopic substitution (Bigeleisen 1955) is that calculated fractionation factors are almost completely insensitive to the number of substituted atoms.

Example calculation: $^{53}Cr \leftrightarrow {}^{50}Cr$ substitution in the chromate anion. An example calculation on the chromate anion $[CrO_4]^{2-}$ makes use of tabulated *G* and *F* matrix elements.

Table 1. Block diagonalized G and F matrices for tetrahedral XY_4 and octahedral XY_6 molecules, using the modified Urey-Bradley force field. Adapted from Nakmoto (1997). m_X and m_Y are the masses of atoms of X and Y, and r is the length of the X-Y bond. K, H, and F_{NB} are force constants for bond stretching, bond-angle bending, and non-bonded repulsion, respectively.

XY_4 molecules, point group T_d

A_1 (ν_1) – Raman active

$G(A_1) = 1/m_Y$ $\quad$ $F(A_1) = (K + 4F_{NB})$

E (ν_2) – doubly degenerate, Raman active

$G(E) = 3/(r^2 m_Y)$ $\quad$ $F(E) = (H + 0.4F_{NB})$

F_2 (ν_3, ν_4) – triply degenerate, Raman and infrared active

$$G(F_2) = \begin{bmatrix} \frac{1}{m_O} + \frac{4}{3m_{Cr}} & \frac{-8}{3m_{Cr}r} \\ \frac{-8}{3m_{Cr}r} & \frac{1}{r^2}\left(\frac{16}{3m_{Cr}} + \frac{2}{m_O}\right) \end{bmatrix} \qquad F(F_2) = \begin{bmatrix} K + \frac{6}{5}F_{NB} & \frac{3}{5}rF_{NB} \\ \frac{3}{5}rF_{NB} & r^2\left(H + 0.4F_{NB}\right) \end{bmatrix}$$

XY_6 molecules, point group O_h

A_{1g} (ν_1) – Raman active

$G(A_1) = 1/m_Y$ $\quad$ $F(A_1) = (K + 4F_{NB})$

E_g (ν_2) – doubly degenerate, Raman active

$G(E_g) = 1/m_Y$ $\quad$ $F(E_g) = (K + 0.7F_{NB})$

F_{1u} (ν_3, ν_4) – triply degenerate, infrared active

$$G(F_{1u}) = \begin{bmatrix} \frac{1}{m_O} + \frac{2}{m_{Cr}} & \frac{-4}{m_{Cr}r} \\ \frac{-4}{m_{Cr}r} & \frac{2}{r^2}\left(\frac{4}{m_{Cr}} + \frac{1}{m_O}\right) \end{bmatrix} \qquad F(F_2) = \begin{bmatrix} K + 1.8F_{NB} & 0.9rF_{NB} \\ 0.9rF_{NB} & r^2\left(H + 0.55F_{NB}\right) \end{bmatrix}$$

F_{2g} (ν_5) – triply degenerate, Raman active

$G(F_{2g}) = 4/(r^2 m_Y)$ $\quad$ $F(F_{2g}) = (H + 0.55F_{NB})$

F_{2u} (ν_6) – triply degenerate, neither Raman nor infrared active

$G(F_{2u}) = 2/(r^2 m_Y)$ $\quad$ $F(F_{2u}) = (H + 0.55F_{NB})$

The chromate anion is a highly soluble, toxic tetrahedral complex (point group T_d) that occurs in oxidized, neutral-basic solutions. It is also one of a small number of aqueous complexes that have been thoroughly characterized by spectroscopic measurements on numerous isotopic compositions (Müller and Königer 1974), so it will be possible to check the vibrational model against real data. Here the MUBFF is applied under the assumption that aqueous chromate can be approximately modeled as a gas-phase molecule.

Due to numerous symmetries in the T_d point group, most of the nine vibrational modes of tetrahedral XY_4 molecules and complexes like the chromate anion are degenerate (meaning that two or more modes have the same frequency), and there are only four distinct frequencies. These frequencies are all observable with Raman spectroscopy, which is particularly suited to studies of dissolved substances. There is one frequency belonging to the A_1 irreducible representation, one belonging to the doubly degenerate E irreducible representation, and two to the triply-degenerate F_2 irreducible representation. F_2 frequencies are also observable with infrared spectroscopy, although water is such a strong infrared absorber that this can be difficult in solution. For the natural isotopic mixture in chromate (dominantly $[^{52}Cr^{16}O_4]^{2-}$) the four distinct frequencies are (Müller and Königer 1974):

$\nu_1(A_1)$, 846 cm^{-1} $\quad$ $\nu_2(E)$, 347 cm^{-1} $\quad$ $\nu_3(F_2)$, 891 cm^{-1} $\quad$ $\nu_4(F_2)$, 368 cm^{-1}

The symmetrized *G* and *F* matrices for $[CrO_4]^{2-}$ molecules are:

$$G = \begin{bmatrix} \frac{1}{m_O} & 0 & 0 & 0 \\ 0 & \frac{3}{m_0 r^2} & 0 & 0 \\ 0 & 0 & \frac{1}{m_O} + \frac{4}{3m_{Cr}} & \frac{-8}{3m_{Cr} r} \\ 0 & 0 & \frac{-8}{3m_{Cr} r} & \frac{1}{r^2}\left(\frac{16}{3m_{Cr}} + \frac{2}{m_O}\right) \end{bmatrix}$$

$$F = \begin{bmatrix} K + 4F_{NB} & 0 & 0 & 0 \\ 0 & r^2\left(H + 0.4F_{NB}\right) & 0 & 0 \\ 0 & 0 & K + \frac{6}{5}F_{NB} & \frac{3}{5}rF_{NB} \\ 0 & 0 & \frac{3}{5}rF_{NB} & r^2\left(H + 0.4F_{NB}\right) \end{bmatrix}$$

where *K*, *H*, and F_{NB} are force constants for Cr-O bond stretching, O-Cr-O bond-angle bending, and O-O repulsion, respectively, and *r* is the equilibrium Cr-O bond length. The first two terms on the diagonals correspond to the A_1 and E vibrations, while the 2×2 submatrix at lower right corresponds to the F_2 vibrations—each can be solved separately:

$$4\pi^2\nu_1^2 = \frac{1}{m_O}\left(K + 4F_{NB}\right)$$

$$4\pi^2\nu_2^2 = \frac{3}{m_O}\left(H + 0.4F_{NB}\right)$$

$$4\pi^2{\nu_{3,4}}^2 = eigenvalue\left(\begin{bmatrix} \frac{1}{m_O} + \frac{4}{3m_{Cr}} & \frac{-8}{3m_{Cr} r} \\ \frac{-8}{3m_{Cr} r} & \frac{1}{r^2}\left(\frac{16}{3m_{Cr}} + \frac{2}{m_O}\right) \end{bmatrix}\begin{bmatrix} K + \frac{6}{5}F_{NB} & \frac{3}{5}rF_{NB} \\ \frac{3}{5}rF_{NB} & r^2\left(H + 0.4F_{NB}\right) \end{bmatrix}\right)$$

Here there are four measured frequencies with which to constrain three independent force constants, so the best-fitting force constants can be determined through an iterative least squares fit, minimizing $\Sigma(\nu_{meas}-\nu_{calc})^2$. Assuming average atomic masses of 51.996 and 15.9994 for chromium and oxygen, respectively, the best-fit force constants are K = 495.2 Newtons/m, H = 21.3 Newtons/m, and F_{NB} = 44.7 Newtons/m. These force constants show the typical relationship $K >> H,F_{NB}$. Calculated frequencies are:

$\nu_1(A_1)$, 845.6 cm^{-1} $\nu_2(E)$, 353.1 cm^{-1} $\nu_3(F_2)$, 891.3 cm^{-1} $\nu_4(F_2)$, 362.5 cm^{-1}

with a total squared misfit of 68 cm^{-2}. If the masses of ^{50}Cr and ^{53}Cr are inserted for m_{Cr}, it is found that only the F_2 frequencies ν_3 and ν_4 change, falling by 7.4 cm^{-1} and 2.8 cm^{-1}, respectively, upon substitution of the heavier isotope. The chromium-isotope sensitivity of the F_2 vibrations occurs because these are the only ones in which the chromium atom moves (Fig. 5). A_1 and E modes, by contrast, consist only of motion of oxygen atoms. Infrared measurements on sulfate salts doped with $[^{50}CrO_4]^{2-}$ and $[^{53}Cr^{16}O_4]^{2-}$ show that the F_2 frequencies actually change by 8.5±0.3 cm^{-1} and 2.2±0.3 cm^{-1}, respectively. We can use both calculated and observed isotopic frequencies to calculate reduced partition function ratios for ^{53}Cr-^{50}Cr exchange in chromates. $\alpha_{Chromate-Cr}$ = 1.0365 and 1.0393 at 298 K, respectively, a difference of 2.8 per mil. Published measurements have reported variations in $^{53}Cr/^{52}Cr$ ratios rather than $^{53}Cr/^{50}Cr$ (Ellis et al. 2002); so it is useful calculate analogous fractionation factors for the ^{53}Cr-^{52}Cr exchange reaction. These are 1.0120 and 1.0129, respectively, suggesting that the MUBFF model introduces an error of ~1 per mil in a room temperature calculation of $^{53}Cr/^{52}Cr$ fractionation.

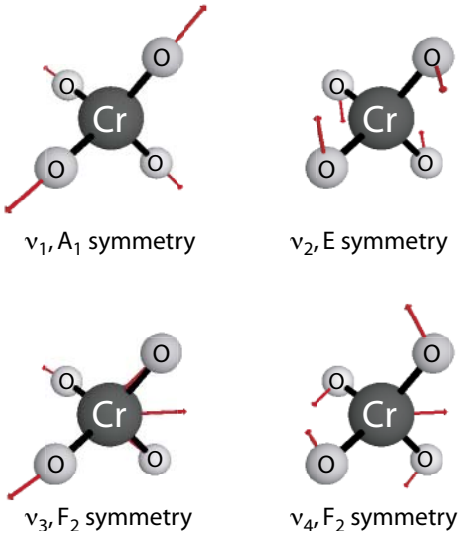

Figure 5. Normal modes for vibration of tetrahedral $[CrO_4]^{2-}$ (chromate). There are four distinct vibrational frequencies, including one doubly-degenerate vibration (E symmetry) and two triply-degenerate vibrations (F_2 symmetry), for a total of nine vibrational modes. Arrows show the characteristic motions of each atom during vibration, and the length of each arrow is proportional to the magnitude of atomic motion. Only F_2 modes involve motion of the central chromium atom, and as a result their vibrational frequencies are affected by Cr-isotope substitution. The normal modes shown here were calculated with an *ab initio* quantum mechanical model, using hybrid Hartree-Fock/Density Functional Theory (B3LYP) and the 6-31G(d) basis set—other *ab initio* and empirical force-field models give very similar results.

Transferable empirical force fields (interatomic potentials)

Other types of models have occasionally been used to calculate unknown vibrational frequencies. One promising approach has been the use of transferable empirical force fields. Transferable force fields are designed to be applicable to a range of compounds, rather than a single molecule, and consequently include parameters that account explicitly for properties like equilibrium bond lengths, ionic charges, and coordination number that change from one substance to another. This flexibility means that transferable force fields (often called interatomic potentials) can also be used to calculate binding, surface and defect energies, and to estimate unknown crystal structures and elastic properties. Interatomic potentials have been developed for numerous oxide, silicate, and carbonate materials (Catlow et al. 1988; Dove et al. 1992; Le Roux and Glasser 1997; Demiralp et al. 1999; Cygan et al. 2002). Much like MUBFF force constants, transferable potentials are determined using experimental measurements of molecular structures, mineral lattice constants and elastic properties, and known vibrational frequencies; they may also be constrained by *ab initio* calculations (Harrison and Leslie 1992). Free and commercial software packages such as GULP (Gale and Rohl 2003) and Cerius 2 (Accelrys) can be used to model vibrational spectra of minerals, molecules, and solutions based on these transferable potentials. The author is not aware of any published theoretical stable isotope studies of non-traditional elements that have taken advantage of transferable force fields, but they have been used in calculations of oxygen and carbon isotope fractionations in silicates (Patel et al. 1991) and carbonate minerals (Dove et al. 1992). An introduction to the construction and use of interatomic potentials was presented in a previous Reviews in Mineralogy and Geochemistry volume (Gale 2001).

Ab initio force-field modeling

Over the last decade, *ab initio* quantum-mechanical force fields have begun to be applied in theoretical stable isotope studies of molecules and dissolved species (Bochkarev et al. 2003; Driesner et al. 2000; Oi 2000; Oi and Yanase 2001). This method shows great promise for future studies, because *ab initio* calculations accurately describe chemical properties such as force constants without the necessity of assuming allowed force-constant types (which may not be universally applicable). *Ab initio* calculations are also ideally suited to molecules with

relatively few known vibrational frequencies because there are no empirical parameters that require fitting. Because the minimum-energy molecular structure is typically also calculated, measured structures can be used to verify the appropriateness of a particular model. Numerous reviews of quantum mechanical calculations (e.g., Foresman and Frisch 1996; Thijssen 1999) and their applications in Earth science (Cygan and Kubicki 2001) have been published.

The central problem in any quantum mechanical model is finding accurate solutions to the time independent form of the Schrödinger equation,

$$\boldsymbol{H}\Psi = E\Psi$$

where Ψ is the wavefunction describing the electronic structure of the molecule, H is the Hamiltonian describing the potential field and kinetic energy of electrons and atomic nuclei (nuclei are generally assumed to be fixed in space), and E are the allowed electronic energies of the molecule. For all but the simplest systems, it is not possible to solve the Schrödinger equation exactly. However, reasonably accurate approximate solutions are possible using simplified descriptions of the electronic potentials and wavefunctions. Regardless of the method chosen, determination of the ground state electronic structure of a molecule involves the optimization of a large number of variables, which are usually determined via an iterative procedure to yield a minimum-energy, self-consistent set of electronic wavefunctions. Numerous free and commercial software packages such as Jaguar (Schrödinger, Inc.), Gaussian (Gaussian, Inc.), and GAMESS (Schmidt et al. 1993) have been developed to make it possible for non-specialists to create quantum-mechanical models of molecules and crystals.

Two common approximation methods are the Hartree-Fock (HF) method (Roothaan 1951) and density functional theory (DFT) (Hohenberg and Kohn 1964; Kohn and Sham 1965). In Hartree-Fock theory, the interactions between different electrons in a molecule are treated in a simplified way. Each electron "sees" other electrons as a time-averaged distribution, ignoring correlations between the positions of electrons in interacting orbitals. More accurate methods that take account of electron correlation have also been developed (Pople et al. 1976). HF calculations are much faster than correlation methods, however, and are often able to provide reasonably accurate descriptions of molecular structures and vibrational properties. HF methods work best for molecules with simple bond structures made up of low atomic-number atoms, and less well for molecules with exotic electronic structures (like O_3) and transition elements. DFT methods are distinguished from HF and correlated methods in their focus on determining electronic energies from the electron density. DFT methods are particularly well suited to crystals and solutions, and often provide a better description of transition-element bearing molecules than HF theory. Hybrid DFT-HF calculations such as the Becke three-parameter Lee-Yang-Parr (B3LYP) method (Becke 1993) are possible, and are commonly used to model molecular structures and vibrational frequencies. In fact B3LYP has become the method of choice for studying large molecules and atomic clusters in chemistry and earth science. Although the HF and DFT methods were developed separately and have different strengths and weaknesses, they have been implemented together in numerous commercial and open-source software packages, i.e. Jaguar (Schrödinger, Inc.), Gaussian (Gaussian, Inc.), and GAMESS (Schmidt et al. 1993), and it is natural to group them together in describing vibrational models. Note that some DFT methods are not strictly *ab initio* because a few empirical parameters (other than fundamental constants like the charge and mass of an electron and the speed of light) are used; these parameters are fixed within a given method however, and are so far removed from the user that the practical distinction is minor. In all of these methods, molecular electronic wavefunctions are typically built up using a set of orbital-like basis functions called a basis set. As with electronic correlation, the choice of basis set is governed by a compromise between accuracy and computational expense. Commonly used basis sets include 6-31G(d) (Francl et al. 1982) and 6-311G(d,p) (Krishnan et al. 1980).

Density functional theory has been extensively used to calculate vibrational properties of minerals and other crystalline phases in addition to molecules and molecule-like substances. This method has recently begun to be used to calculate isotope fractionation factors (Schauble et al. in press; Anbar et al. in press), and shows great potential for future research. Programs such as ABINIT (Gonze et al. 2002), pwSCF (Baroni et al. 2001)—both freely available—and the commercial package CASTEP (Accelrys, Inc.) can be used to calculate vibrational properties of crystals.

The Schrödinger equation can also be solved semi-empirically, with much less computational effort than *ab initio* methods. Prominent semi-empirical methods include MNDO, AM1, and PM3 (Dewar 1977; Dewar et al. 1985; Stewart 1989a; Stewart 1989b). The relative computational simplicity of these methods is accompanied, however, by a substantial loss of accuracy (Scott and Radom 1996), which has limited their use in geochemical simulations. Historically, semi-empirical calculations have also been limited by the elements that could be modeled, excluding many transition elements, for example. Semi-empirical calculations have been used to predict Si, S, and Cl isotopic fractionations in molecules (Hanschmann 1984), and these results are in qualitative agreement with other theoretical approaches and experimental results.

There are typically three steps in creating an *ab initio* quantum-mechanical model of a molecule. In the first step, the minimum-energy static structure of the molecule is determined via geometric relaxation. From an initial guess geometry, often the experimentally determined structure of the molecule, the forces on each atom are calculated, and a refined guess structure is determined. This procedure continues iteratively until the residual forces acting on each atom are sufficiently small—typically on the order of 10^{-10} Newtons or less. HF, DFT, and hybrid HF-DFT *ab initio* methods can be expected to reproduce experimental bond lengths and angles to within approximately 2 pm (0.02 Å) and 1º–2º, respectively, when the chosen method and basis set are appropriate. Once the minimum-energy configuration has been calculated, the second step is the determination of force constants for displacements of the atomic nuclei from their minimum energy positions. Finally, unknown frequencies are determined by a calculation with the appropriate isotopic masses. Since the force constants are not affected by isotopic substitution, this final step involves much less computational effort than the preceding two. Vibrational frequencies for numerous isotopic configurations of a molecule can be calculated quickly once the matrix of force constants has been determined, even for relatively complex substances.

It important to note that *ab initio* force fields of all types tend to make systematic errors in calculating vibrational frequencies (Pople et al. 1993; Scott and Radom 1996; Wong 1996). With HF calculations using the 6-31G(d) basis set, for instance, vibrational frequencies of gas-phase molecules are typically overestimated by about 12%, with both high- and low-frequency vibrations off by roughly the same scale factor (Scott and Radom 1996). Some gas-phase scale factors for other *ab initio* methods are given in Table 2. In cases where the *ab initio* molecular structure is close to the observed structure (angles within 1–2º, bond lengths within 2 pm) and calculated vibrational frequencies are related to observed frequencies by a uniform scaling factor, the ratios of frequencies of isotopic molecules should be accurately predicted (Schauble et al. 2003). For substances with relatively well-known vibrational spectra, model frequency ratios can be normalized to observed frequencies in the same way as MUBFF model frequencies.

Example calculation: $^{37}Cl \leftrightarrow {}^{35}Cl$ substitution in methyl chloride. Here we will create an *ab initio* vibrational model of CH_3Cl, a tetrahedral molecule with a less symmetric structure (point group C_{3v}) than chromate. Low-symmetry molecules can be tedious and difficult to model with empirical methods because of the large number of force-constant parameters that need to be constrained (although methyl chloride is small enough that such calculations

Table 2. Scale factors for *ab initio* model vibrational frequencies adapted from (Scott and Radom 1996). Please note that these scale factors are determined by comparing model and measured frequencies on a set gas-phase molecules dominated by molecules containing low atomic-number elements (H-Cl). These scale factors may not be appropriate for dissolved species and molecules containing heavier elements, and it is always a good idea to directly compare calculated and measured frequencies for each molecule studied. The root-mean-squared (rms) deviation of scaled model frequencies relative to measured frequencies is also shown, giving an indication of how reliable each scale factor is.

Method	Basis set	Scale factor	rms deviation (cm^{-1})
HF	3-21G	0.9085	87
HF	6-31G(d)	0.8953	50
HF	6-31G(d,p)	0.8992	53
HF	6-311G(d,p)	0.9051	54
B3LYP	6-31G(d)	0.9614	34

are feasible). Low-symmetry molecules are ideal candidates for *ab initio* modeling, which eliminates the time-consuming and error-prone process of fitting empirical parameters to measured frequencies. Calculations in this example are made using the open-source software package GAMESS (Schmidt et al. 1993), which can be downloaded without cost by academic and commercial users (*http://www.msg.ameslab.gov/GAMESS/GAMESS.html*). Hartree-Fock calculations appear to provide reasonably accurate models of the effects of isotopic substitution on vibrational frequencies of chlorocarbons and hydrochlorocarbons (Schauble et al. 2003), and are computationally fast. Here we will perform a Hartree-Fock calculation using the medium-accuracy 6-31G(d) basis set. As an initial guess for the structural relaxation step we can take the experimentally determined structure (Fig. 6), which has a C-Cl bond length of 177.6 pm, C-H bond lengths of l08.5 pm, and H-C-H bond angles of 110.4º (Jensen 1981). Geometry optimization takes <1 minute on a Macintosh desktop computer with a 400 MHz G4 processor, and yields a structure very close to what is observed: r(C-Cl) = 178.5 pm, r(C-H) = 107.8 pm, and ∠(H-C-H) = 110.5º. The total calculated electronic energy is –499.093153 Hartrees (–1,310,367.75 kJoules/mole).

Using the optimized structure, the vibrational frequencies are calculated. By default, GAMESS assumes that the dominant isotopic form of CH_3Cl ($^{12}C^1H_3{}^{35}Cl$) is present. GAMESS does not automatically classify vibrations by symmetry. However, this task can be accomplished by visual inspection using molecule animation software like MacMolPlt (Bode

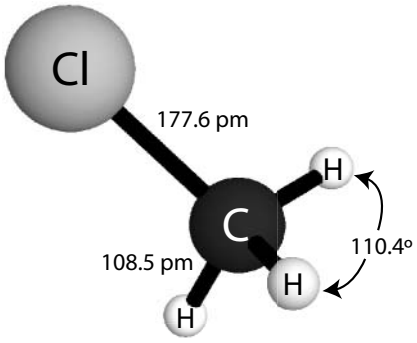

Figure 6. Measured molecular structure of methyl chloride (CH_3Cl), taken from Jensen (1981). CH_3Cl is a nearly tetrahedral molecule with C_{3v} symmetry. All C-H bond lengths, H-C-H angles and H-C-Cl angles are identical.

and Gordon 1998) and symmetry character tables found in many spectroscopy and inorganic chemistry textbooks (e.g., Nakamoto 1997; Shriver 1999). Methyl chloride is particularly simple because all doubly degenerate vibrations have E symmetry, and all remaining vibrations have A_1 symmetry. Calculated and measured frequencies are compared in Table 3. Measured frequencies are consistently ~10% lower than *ab initio* frequencies, in good agreement with the standard HF/6-31G(d) scale factor (Scott and Radom 1996).

^{37}Cl is sufficiently common that some vibrational frequencies of isotopically heavy methyl chloride have been measured spectroscopically, so it is possible to compare measured and model frequency shifts. It is found that ν_3 and ν_6 are the only frequencies that shift significantly when ^{37}Cl is substituted for ^{35}Cl; the model estimates that the ratio of ν_3 in $^{12}C^{1}H_3{}^{37}Cl$ divided by the frequency in $^{12}C^{1}H_3{}^{35}Cl$ is 0.9919, for ν_6 the ratio is 0.9996. These ratios are in excellent agreement with measured ratios of 0.9920 and 0.9996, respectively. Using normalized model frequencies (Eqn. 6), $\alpha_{\text{Methyl Chloride–Cl}} = 1.0088$ at 298 K.

Table 3. Measured (Black and Law 2001) and *ab initio* vibrational frequencies for methyl chloride, $^{12}C^{1}H_3{}^{35}Cl$. *Ab initio* frequencies are calculated with GAMESS, using the Hartree-Fock method and 6-31G(d) basis set. The ratio of each measured and model frequency is also shown.

Vibration	Measured frequency (cm^{-1})	*Ab initio* frequency (cm^{-1})	Meas./*Ab init.* Ratio	ν_{37}/ν_{35} (*ab initio*)
ν_1 (A_1)	2953.9	3267.33	0.9041	1.00000
ν_2 (A_1)	1354.88	1538.08	0.8809	0.99991
ν_3 (A_1)	732.84	782.60	0.9364	0.99194
ν_4 (E)	3039.29	3371.02	0.9016	1.00000
ν_5 (E)	1452.18	1628.96	0.8915	0.99999
ν_6 (E)	1018.07	1138.36	0.8943	0.99961

Theoretical applications of Mössbauer spectroscopy

The first theoretical calculations of stable isotope fractionation factors in the iron isotope system were based on Mössbauer spectroscopy rather than traditional vibrational spectroscopy (Polyakov 1997; Polyakov and Mineev 2000). These early studies successfully predicted that measurable equilibrium fractionations occur between different iron-bearing minerals, and that Fe^{3+}-bearing phases will tend to have higher $^{57}Fe/^{54}Fe$ than coexisting Fe^{2+}-bearing phases (Beard et al. 2003). However, predicted fractionations between different Fe^{2+}-bearing oxides appear to be larger than is observed in experimentally equilibrated phases and suites of natural samples. The source of disagreement between predicted Fe-isotope fractionations and experimental results has not yet been identified, but may lie in the extensive data modeling and processing required to predict fractionations from measured Mössbauer spectra.

Mössbauer spectroscopy involves the measurement of minute frequency shifts in the resonant gamma-ray absorption cross-section of a target nucleus (most commonly ^{57}Fe; occasionally ^{119}Sn, ^{197}Au, and a few others) embedded in a solid material. Because Mössbauer spectroscopy directly probes the chemical properties of the target nucleus, it is ideally suited to studies of complex materials and Fe-poor solid solutions. Mössbauer studies are commonly used to infer properties like oxidation states and coordination number at the site occupied by the target atom (Hawthorne 1988). Mössbauer-based fractionation models are based on an extension of Equations (4) and (5) (Bigeleisen and Mayer 1947), which relate α to either sums of squares of vibrational frequencies or a sum of force constants. In the Polyakov (1997)

formulation, the fractionation factor is related directly to the average vibrational kinetic energy, $<KE>$, of atoms of the element of interest (the brackets indicate an averaged atomic thermodynamic quantity):

$$\ln(\alpha_{XR-X}) = \frac{\Delta m_X}{m_{heavy_X}}\left(\frac{\langle KE_X \rangle}{kT} - \frac{3}{2}\right)$$

where the figure of 3/2 in parentheses represents classical thermal kinetic energy. Mössbauer spectroscopy can be used to estimate $<KE_X>$ via the second-order Doppler shift (SOD), an extremely small but measurable shift of the observed resonant frequency. Unlike conventional Doppler shifts, which are caused by line-of-sight motion, SOD results from the relativistic time dilation of the Mössbauer nucleus as it vibrates perpendicular to the line of sight between the gamma-ray source and the absorbing atom. In any iron-bearing crystal, ^{57}Fe atoms bound in the crystal lattice vibrate about their equilibrium positions, each with a finite velocity, v. Because it is moving, special relativity dictates that each atom has a slightly slower internal clock than an observer at rest. A photon that appears to a ^{57}Fe nucleus to have a frequency ν will appear to the observer as a photon with a frequency equal to $\nu+\delta\nu$, where

$$\frac{\delta\nu}{\nu} = \frac{1}{\sqrt{1+\frac{v^2}{c^2}}} - 1 \approx -\frac{v^2}{2c^2}$$

So by measuring the second-order Doppler shift of the Mössbauer nuclei in a material it is possible to determine their average velocity $<v^2>$ and thus their average vibrational kinetic energy, $<KE_X> = m_{Mossbauer_X}<v^2>/2$, where $m_{Mossbauer_X}$ is the mass of the Mössbauer nucleus. The magnitude S of a measured SOD is typically reported in terms of an equivalent conventional Doppler shift (relative velocity between gamma-ray source and absorber),

$$S = \frac{\delta\nu}{\nu}c$$

Using this convention, the Mössbauer model expression for equilibrium isotopic fractionation becomes:

$$\ln(\alpha_{XR-X}) = \frac{\Delta m_X}{m_{heavy_X}}\left(\frac{m_{Mossbauer_X} Sc}{kT} - \frac{3}{2}\right)$$

(Polyakov 1997). Because the second-order Doppler shift is not the only factor controlling Mössbauer absorption frequencies, it is generally necessary to process data taken at a variety of temperatures, and to make a number of assumptions about the invariance of other factors with temperature and the form and properties of the vibrational density of states of the Mössbauer atom. Principles involved in analyzing temperature dependencies in Mössbauer spectra are extensively discussed in the primary literature (Hazony 1966; Housley and Hess 1966; Housley and Hess 1967) and reviews (e.g., Heberle 1971).

Integrating theoretically estimated fractionations with measurements

It should be clear from the preceding discussions that practical application of equilibrium stable isotope fractionation theory often requires a certain amount of simplification of complex and poorly studied systems. Given this reality, one should not be surprised to find that theoretically determined equilibrium fractionations rarely achieve accuracies approaching the nominal precisions of measurements made with modern analytical techniques. It should

noted that future developments in vibrational modeling, particularly in *ab initio* force-field calculations and the evaluation of solvent effects, are likely to narrow the accuracy gap. The most important point, however, is that even simplified theoretical calculations have a number of powerful advantages. For instance, rough estimates can be particularly useful in developing a wide-ranging theoretical framework to help guide initial experimental investigations. In addition, theoretical calculations can greatly enhance the impact of limited experimental data, even when the former is much less accurate. They help constrain fractionation mechanisms in natural samples and experimental run products where it may not be clear that equilibrium has been attained (Fig. 7)—qualitative agreement between theoretical and observed fractionations, particularly when observed over a range of temperatures, constitutes a powerful argument in favor of the experimental attainment of equilibrium. Finally, theoretical calculations can be used to extend experimentally calibrated fractionations to low temperatures where isotopic exchange is too slow to reach equilibrium on a reasonable laboratory timescale (Clayton and Kieffer 1991).

BASIC KINETIC STABLE ISOTOPE FRACTIONATION THEORY

Kinetic fractionations can occur when there is incomplete isotopic exchange between the different phases present in a system. A thorough introduction to kinetic stable isotope fractionation theory is unfortunately beyond the scope of the present review. However, it is useful to include a brief discussion of some basic aspects, particularly in comparison to equilibrium fractionation theory. A simple example of kinetic fractionation is the evaporation of a liquid water droplet into a vacuum, in this example H_2O molecules entering the gas phase are physically removed from the vicinity of the droplet, so there is no chance for isotopic equilibration between vapor-phase molecules and the residual liquid. Isotopic fractionation in this case is determined by a one-way reaction path, and will not, in general, be the same as the fractionation in a system where vapor-phase molecules are able to equilibrate and exchange with the liquid. In other reactions, isotopic exchange is limited by an energy barrier—an

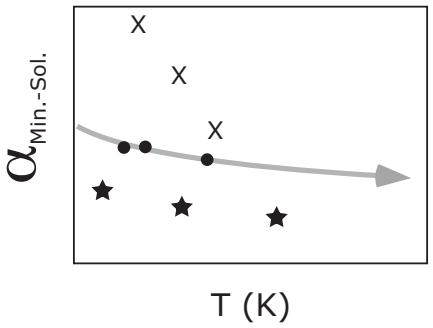

Figure 7. Using a theoretically determined equilibrium fractionation to interpret measured isotopic fractionations in a hypothetical mineral-solution system. Three sets of data are shown. The theoretical equilibrium fractionation for this system is indicated by the gray arrow. The first set of data, indicated by circles, closely follow the calculated fractionation, suggesting a batch equilibrium fractionation mechanism. The second set of data (stars) is displaced from the theoretical curve. This may either indicate a temperature-independent kinetic fractionation superimposed on an equilibrium-like fractionation, or that the theoretical calculation is somewhat inaccurate. The third set of data (crosses) shows much greater temperature sensitivity than the equilibrium calculation; this provides evidence for a dominantly non-equilibrium fractionation mechanism. For the first data set, the theoretical fractionation curve can be used to extrapolate beyond the measured temperature range. The second data set can also be extrapolated along a scaled theoretical curve (Clayton and Kieffer 1991).

exchange activation energy—that must be surmounted in order for two atoms with different masses to swap positions (Fig. 8).

The size of the activation energy for isotopic exchange reflects the need to break bonds and rearrange atoms in order to effect exchange. The rate at which atoms are exchanged decreases with increasing height of the energy barrier, increases with temperature, and also depends on geometric constraints. In natural systems, and particularly at low temperatures, kinetic stable isotope fractionations are common. With non-traditional stable isotope systems we are typically interested in heavier elements and condensed phases; for these the most common types of kinetic fractionations are likely to be those driven by the effects of isotopic mass on molecular and atomic velocities and diffusivity, and by isotopic effects on activation energies. Other mechanisms can be important in gas-phase and very low-temperature reactions, but are largely beyond the scope of the present work.

Effects of isotopic mass on molecular and atomic velocities and diffusivity

In a gas with a well defined temperature, the translational kinetic energies of all molecules are the same, on average,

$$\langle KE \rangle = \frac{3}{2} \mathrm{k}T = \frac{1}{2} m \left\langle \mathrm{v}^2 \right\rangle$$

where m here is the mass of the molecule and v is its velocity. It is apparent that molecules having different isotopic compositions will have different average velocities,

$$\frac{\left\langle v_{heavy}{}^2 \right\rangle}{\left\langle v_{light}{}^2 \right\rangle} = \frac{m_{light}}{m_{heavy}}$$

For fractionation processes that are chiefly dependent on molecular velocity, this relationship can be rearranged into a simple translational isotopic fractionation factor,

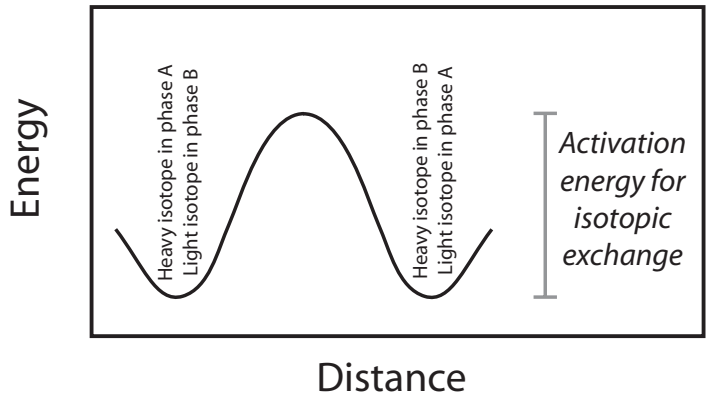

Figure 8. Schematic diagram of the potential energy trajectory of an isotope exchange reaction. In general, isotopic exchange requires the rearrangement or breaking of chemical bonds, which involves an increase in the potential energy of the molecule. This activation energy limits the rate at which exchange can take place, particularly at low temperatures. Equilibrium isotopic fractionation requires isotopic exchange, kinetic fractionations can occur if molecules are unable to surmount the exchange energy barrier. For simplicity isotopic effects on exchange energy are ignored.

$$\alpha_{XR(translation)} = \sqrt{\frac{m_{heavy_{XR}}}{m_{light_{XR}}}}$$

A good example of translational fractionation is one-way diffusion through an orifice that is smaller than the mean-free path of the gas. Related, but somewhat more complex velocity-dependent fractionations occur during diffusion through a host gas, liquid, or solid. In these fractionations the isotopic masses in the translational fractionation factor are often replaced by some kind of effective reduced mass. For instance, in diffusion of a trace gas *XR* through a medium, *Y*, consisting of molecules with mass m_Y,

$$\frac{D_{light_{XR}}}{D_{heavy_{XR}}} = \sqrt{\frac{\mu_{heavy_{XR-Y}}}{\mu_{light_{XR-Y}}}} = \sqrt{\frac{\frac{1}{m_{light_{XR}}} + \frac{1}{m_Y}}{\frac{1}{m_{heavy_{XR}}} + \frac{1}{m_Y}}}$$

where $D_{light_{XR}}$ and $D_{heavy_{XR}}$ are the diffusivities of the isotopically light and heavy forms of *XR*, respectively (Reid et al. 1977). Such diffusivity ratios will always be closer to unity than the simple translational fractionation factor.

Effects of isotopic mass on rates of activation

In many chemical processes the rate of reaction depends chiefly on one particular transformative step. Under conditions where reaction products are not able to back-exchange with the reactants, this rate-limiting step also can control the isotopic fractionation between reactants and products. For simple reactions where one molecule dissociates, a transition state theory of isotopic fractionation has been developed (Eyring 1935; Bigeleisen 1949). In this simplified method of calculating isotopic effects on reaction rates, only the energy barrier between the reactants and a single rate-limiting transition-state is considered. A reaction coordinate, defined as the lowest-energy path from the ground states of the reactants to the transition state, describes the mechanical and electronic distortions necessary before a reaction can take place (Fig. 9). In this theory, the rate at which reactant molecules achieve the transition-state (and thus react to form products) is determined by the statistical probability of a molecule possessing enough energy to reach the summit of the energy barrier,

$$p(E_A) = \exp\left(\frac{-E_A}{\mathrm{k}T}\right)$$

In theory, E_A is the activation energy (the height of the rate-limiting energy barrier in Joules/molecule). This probability is then multiplied by the rate at which reactant molecules sample the reaction coordinate. At the top of the energy barrier, the potential energy curve becomes flat, so that motion across the summit is rather similar to a free translation, rather than a vibrational mode. As a result, the activated molecule has three translational degrees of freedom, one reactive translational degree of freedom, and 3*N*–7 vibrational degrees of freedom (3*N*–6 for a linear molecule). The energies of the reactants and the activated molecules can be determined by evaluating partition functions, using a translational partition function to evaluate the reaction coordinate in the activated molecule. Instead of using the molecular masses, however, an effective reduced mass of molecular motion along the coordinate is used,

$$Q_{Rxn\ Coordinate} = V\left(\frac{2\pi\mu_{Rxn}\mathrm{k}T}{\mathrm{h}^2}\right)^{3/2}$$

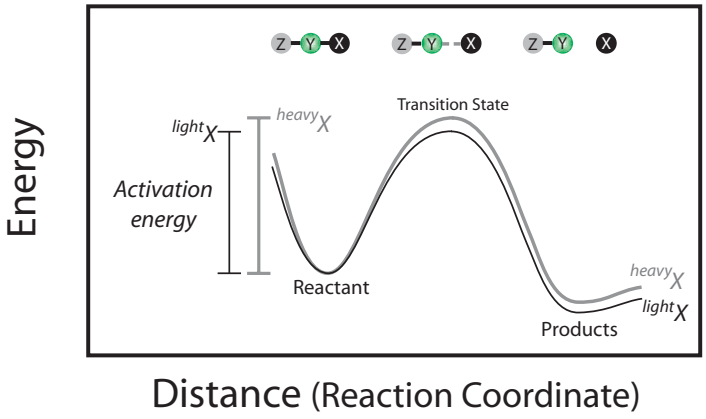

Figure 9. Schematic diagram of the potential energy trajectory of a molecular dissociation reaction. As with the isotopic exchange reaction, the molecule must acquire enough energy in the reaction coordinate to surmount an energy barrier. In this case the dissociating molecule, *ZYX*, splits into two fragments *ZY* and *X*, and the reaction coordinate is roughly equivalent to the length of the *X*-*Y* bond. Typically, the size of this activation energy barrier is slightly affected by isotopic substitution due to differences between the zero-point vibrational energies in the reactant molecule in the ground state and activated state. Here the potential energy curve for a molecule containing the light isotope of element X (^{light}X) is shown in black, and the corresponding curve for a molecule containing a heavier isotope of element X (^{heavy}X) is shown in grey. For clarity, both trajectories are set so that the potential energies of the reactant molecules are the same. In this simple example, the activation energy for the isotopically light molecule is smaller than for the isotopically heavy molecule. In addition, the isotopically light molecule will tend to sample the trajectory faster than the isotopically heavy molecule. For both reasons, the ^{light}X-bearing molecule will tend to react faster than the ^{heavy}X-bearing molecule.

For a simple decomposition reaction of a diatomic molecule, $AB \rightarrow A + B$, μ_{Rxn} is simply

$$\mu_{Rxn} = \frac{m_A m_B}{m_A + m_B}$$

In more complex reactions, it may not be as straightforward to determine the reduced mass along the reaction coordinate because the exact reaction mechanism is poorly known. This task can be facilitated by *ab initio* and empirical force-field software packages with built-in capacities to predict and evaluate reaction coordinates (Schmidt et al. 1993; Gale and Rohl 2003). Once the relevant reduced masses are known, a derivation similar to Urey's (1947) equation for equilibrium isotopic fractionation can be followed, obtaining:

$$\alpha_{transition-XR} = \frac{\mu_{heavy_{XR(Rxn)}}}{\mu_{light_{XR(Rxn)}}} \frac{\alpha_{XR(activated)-X}}{\alpha_{XR-X}}$$

where $\alpha_{transition-XR}$ is the ratio of reaction rates of $^{heavy}XR$ and $^{light}XR$, $\mu_{heavy_{XR(Rxn)}}$ and $\mu_{light_{XR(Rxn)}}$ are the effective reduced masses for motion along the reaction coordinate for the two isotopic forms of *XR*, $\alpha_{XR\text{-}X}$ for the reactant is calculated using Equation (3), and $\alpha_{XR(activated)}$ for the activated molecule is calculated using Equation (3) using the $3N-7$ vibrational modes of the activated complex. This method has been applied in theoretical studies of isotopic fractionations in non-traditional systems (e.g., Krouse and Thode 1962; Paneth 2003). The Paneth (2003) study predicts kinetic chlorine-isotope fractionations in reasonable agreement with experimental measurements.

MASS-DEPENDENCE OF EQUILIBRIUM AND KINETIC ISOTOPE FRACTIONATIONS

Recent discoveries of oxygen and sulfur fractionations (e.g., Farquhar et al. 2000; Thiemens et al. 2001) that appear to have unusual mass dependence has renewed interest in variations in the mass dependence of different fractionation mechanisms (Gao and Marcus 2002; Young et al. 2002). Usually, mass-dependent fractionations scale in proportion to differences in isotopic mass:

$$\frac{({}^{i_X}/_{k_X})\alpha - 1}{({}^{j_X}/_{k_X})\alpha - 1} \approx \frac{m_{i_X} - m_{k_X}}{m_{j_X} - m_{k_X}}$$

where ${}^{(i_X/k_X)}\alpha$ is the fractionation factor separating isotopes ${}^{i}X$ and ${}^{k}X$ in some reaction or process, ${}^{(j_X/k_X)}\alpha$ is the fractionation factor for isotopes ${}^{j}X$ and ${}^{k}X$ in the same reaction, and m_{i_X}, m_{j_X}, and m_{k_X} are the masses of isotopes ${}^{i}X$, ${}^{j}X$, and ${}^{k}X$ respectively. Recent measurements in non-traditional stable isotope systems, including those described in this volume, appear to confirm that mass-dependent fractionation is the norm in geochemical processes and typical chemical reactions. Accurate mass-scaling laws can help to verify whether an observed fractionation has a mass-independent component. In addition, theoretical calculations suggest that different mass-dependent fractionation mechanisms will follow slightly different mass-scaling laws, so that it may be possible, for instance, to distinguish kinetic and equilibrium fractionations (Young et al. 2002). Young et al. (2002) derived and tabulated mass-scaling laws for several types of kinetic and equilibrium fractionations. For equilibrium fractionations,

$$\frac{\ln\left({}^{(i_X/k_X)}\alpha\right)}{\ln\left({}^{(j_X/k_X)}\alpha\right)} = \frac{\left(\frac{1}{m_k} - \frac{1}{m_i}\right)}{\left(\frac{1}{m_k} - \frac{1}{m_j}\right)}$$

This equation follows from the Bigeleisen and Mayer (1947) expression for equilibrium fractionation (Eqn. 4), and is appropriate at high temperatures ($h\nu/kT \leq 5$). This relation may not be accurate at low temperatures, especially near "crossovers" where fractionations switch direction (Matsuhisa et al. 1978; Deines 2003). As the equilibrium fractionation between two substances becomes small near a crossover, the mass-scaling law becomes strongly temperature dependent, and reduced partition function ratios calculated using Equation (3) should be used to estimate mass scaling. For elements other than H, C, N, and O, however, high atomic mass and relatively low vibrational frequencies are expected to make the high-temperature mass-scaling law accurate under most conditions. Anomalous equilibrium mass scaling has never been definitively observed, it may be most likely to occur when one equilibrated phase is a small, highly covalent molecule (e.g., SiC, SeO_3).

For translational kinetic fractionations dependent on molecular velocities, a slightly different relation holds (Young et al. 2002),

$$\frac{\ln\left({}^{(i_X/k_X)}\alpha\right)}{\ln\left({}^{(j_X/k_X)}\alpha\right)} = \frac{\ln\left(\frac{m_{k_{XR}}}{m_{i_{XR}}}\right)}{\ln\left(\frac{m_{k_{XR}}}{m_{j_{XR}}}\right)}$$

where $m_{k_{XR}}$, etc. are the masses of isotopically substituted molecules. Using the simplified

transition state theory of Bigeleisen (1949), a somewhat more complex expression is obtained for fractionations controlled by activation rates,

$$\frac{\ln\left(\left({}^{i_X}/_{k_X}\right)\alpha\right)}{\ln\left(\left({}^{j_X}/_{k_X}\right)\alpha\right)} = \frac{\ln\left(\dfrac{\mu_{k_{XR(Rxn)}}}{\mu_{i_{XR(Rxn)}}}\right)}{\ln\left(\dfrac{\mu_{k_{XR(Rxn)}}}{\mu_{j_{XR(Rxn)}}}\right)}$$

where $\mu_{i_{XR(Rxn)}}$, $\mu_{j_{XR(Rxn)}}$ and $\mu_{k_{XR(Rxn)}}$ are the isotopic reduced masses along the relevant reaction coordinate. This formulation assumes that the activation energy is not significantly affected by isotopic substitution.

CONCLUSIONS

The purpose of this chapter is to provide a concise, comprehensible introduction to the theory of stable isotope fractionations. While many of the fundamental principles discussed here have been understood for decades, applications have been limited by incomplete knowledge of the vibrational properties and reaction mechanisms for all but the simplest gas-phase molecules. Recent developments in theoretical chemistry and spectroscopy are widening the scope of materials and processes that can be studied, however. In particular, *ab initio* methods and transferable empirical potentials are now routinely used to model the vibrational properties of molecules, crystals, and aqueous species with ever increasing precision and reliability; these methods hold great promise for estimating unknown vibrational frequencies of isotopically substituted materials, and for determining potential energy surfaces relevant to chemical reactions. At present these developments are just beginning to be used to full advantage, so that there is a major gap between our ability to measure stable isotope fractionations and our understanding of the processes that cause fractionations to occur. New studies are particularly important now, as novel measurement techniques rapidly expand the scope of stable isotope geochemistry.

ACKNOWLEDGMENTS

This chapter was improved by thoughtful suggestions from E.A. Johnson, T. Chacko, A. D. Anbar, J. R. O'Neil and C. M. Johnson. I would also like to thank H. P. Taylor, Jr. for introducing me to stable isotope fractionation theory, and G. R. Rossman for making vibrational spectroscopy fun.

REFERENCES

Anbar AD, Jarzecki A, Spiro T (in press) Theoretical investigation of iron isotope fractionation between $Fe(H_2O)_6^{3+}$ and $Fe(H_2O)_6^{2+}$. Geochim Cosmochim Acta

Angus WR, Bailey CR, Hale JB, Ingold CK, Leckie AH, Raisin CG, Thompson JW, Wilson CL (1936) Structure of benzene. Part VIII. Assignment of vibration frequencies of benzene and hexadeuterobenzene. J Chem Soc (London):971-987

Barling J, Arnold GL, Anbar AD (2001) Natural mass-dependent variation in the isotopic composition of molybdenum. Earth Planet Sci Lett 193:447-457

Baroni S, de Gironcoli S, Dal Corso A, Giannozzi P (2001) Phonons and related crystal properties from density-functional perturbation theory. Rev Modern Phys 73:515-562

Basile LJ, Ferraro JR, LaBonville P, Wall MD (1973) A study of force fields for tetrahedral molecules and ions. Coord Chem Rev 11:21-69

Beard BL, Johnson CM, Skulan JL, Nealson KH, Cox L, Sun H (2003) Application of Fe isotopes to tracing the geochemical and biological cycling of Fe. Chem Geol 195:87-117

Becke AD (1993) Density-functional thermochemistry. III. The role of exact exchange. J Chem Phys 98: 5648-5652

Bigeleisen J (1949) The relative velocities of isotopic molecules. J Chem Phys 17:675-678

Bigeleisen J (1955) Statistical mechanics of isotopic systems with small quantum corrections. I. General considerations and the rule of the geometric mean. J Chem Phys 23:2264-2267

Bigeleisen J (1998) Second-order correction to the Bigeleisen-Mayer equation due to the nuclear field shift. Proc National Acad Sci 95:4808-4809

Bigeleisen J, Mayer MG (1947) Calculation of equilibrium constants for isotopic exchange reactions. J Chem Phys 15:261-267

Black GM, Law MM (2001) The general harmonic force field of methyl chloride. J Mol Spectrosc 205:280-285

Bochkarev AV, Trefilova AN, Tsurkov NA, Klinskii GD (2003) Calculations of beta-factors by *ab initio* quantum-chemical methods. Russian J Phys Chem 77:622-626

Bode BM, Gordon MS (1998) MacMolPlt: a graphical user interface for GAMESS. J Mol Graphics and Modeling 16:133-138

Bottinga Y (1968) Calculations of fractionation factors for carbon and oxygen isotope exchange in the system calcite-carbon dioxide-water. J Phys Chem 72:800-808

Bullen TD, White AF, Childs CW, Vivit DV, Schulz MS (2001) Demonstration of significant abiotic iron isotope fractionation in nature. Geology 29:699-702

Burkholder JB, Hammer PD, Howard CJ, Maki AG, Thompson G, Chackerian CJ (1987) Infrared measurements of the ClO radical. J Mol Spectrosc 124:139-161

Catlow CRA, Freeman CM, Islam MS, Jackson RA, Leslie M, Tomlinson SM (1988) Interatomic potentials for oxides. Phil Mag A 58:123-141

Chacko T, Cole DR, Horita J (2001) Equilibrium oxygen, hydrogen and carbon isotope fractionation factors applicable to geologic systems. Rev Mineral Geochem 43:1-82

Chacko T, Mayeda TK, Clayton RN, Goldsmith JR (1991) Oxygen and carbon isotope fractionation between CO_2 and calcite. Geochim Cosmochim Acta 55:2867-2882

Clayton RN, Kieffer SW (1991) Oxygen isotopic thermometer calculations. *In*: Stable Isotope Geochemistry: A Tribute to Samuel Epstein, Special Publication No. 3. Taylor HPJ, O'Neil JR, Kaplan IR (eds) The Geochemical Society, San Antonio, Texas, p 1-10

Cotton FA (1971) Chemical Applications of Group Theory. Wiley-Interscience, New York

Criss RE (1991) Temperature dependence of isotopic fractionation factors. *In*: Stable Isotope Geochemistry: A Tribute to Samuel Epstein, Special Publication No. 3. Taylor HPJ, O'Neil JR, Kaplan IR (eds) The Geochemical Society, San Antonio, Texas, p 11-16

Criss RE (1999) Principles of stable isotope distribution. Oxford University Press, New York

Cygan RT, Kubicki JD (2001) Molecular Modeling Theory: Applications in the Geosciences. Reviews in Mineralogy and Geochemistry, Vol. 42, Mineralogical Society of America, Washington, D. C.

Cygan RT, Wright K, Fisler DK, Gale JD, Slater B (2002) Atomistic models of carbonate minerals: bulk and surface structures, defects, and diffusion. Mol Simul 28:475-495

Davis AM, Hashimoto A, Clayton RN, Mayeda TK (1990) Isotope mass fractionation during evaporation of Mg_2SiO_4. Nature 347:655-658

Decius JC (1948) A tabulation of general formulas for inverse kinetic energy matrix elements in acyclic molecules. J Chem Phys 16:1025-1034

Deines P (2003) A note on intra-elemental isotope effects and the interpretation of non-mass-dependent isotope variations. Chem Geol 199:179-182

Demiralp E, Cagin T, Goddard WA (1999) Morse stretch potential charge equilibrium force field for ceramics: Application to the quartz-stishovite phase transition and to silica glass. Phys Rev Lett 82:1708-1711

Dewar MJS (1977) Ground states of molecules. The MNDO method. Approximations and parameters. J Am Chem Soc 99:4899-4907

Dewar MJS, Zoebisch EG, Healy EF, Stewart JJP (1985) The development and use of quantum-mechanical molecular-models. 76. AM1 - a new general-purpose quantum-mechanical molecular-model. J Am Chem Soc 107:3902-3909

Dove MT, Winker B, Leslie M, Harris MJ, Salje EKH (1992) A new interatomic potential model for calcite: Applications to lattice-dynamics studies, phase-transformations, and isotope fractionation. Am Mineral 77:244-250

Driesner T, Ha TK, Seward TM (2000) Oxygen and hydrogen isotope fractionation by hydration complexes of Li^+, Na^+, K^+, F^-, Cl^-, and Br^-: A theoretical study. Geochim Cosmochim Acta 64:3007-3033

Driesner T, Seward TM (2000) Experimental and simulation study of salt effects and pressure/density effects on oxygen and hydrogen stable isotope liquid-vapor fractionation for 4-5 molal aqueous NaCl and KCl solutions to 400 degrees C. Geochim Cosmochim Acta 64:1773-1784

Eggenkamp HGM, Kreulen R, Van Groos AFK (1995) Chlorine stable isotope fractionation in evaporites. Geochim Cosmochim Acta 59:5169-5175

Elcombe MM, Pryor AW (1970) The lattice dynamics calcium fluoride. J Phys C 3:492-499

Eyring H (1935) The activated complex in chemical reactions. J Chem Phys 3:107-117

Farquhar J, Bao HM, Thiemens M (2000) Atmospheric influence of Earth's earliest sulfur cycle. Science 289: 756-758

Foresman JB, Frisch A (1996) Exploring chemistry with electronic structure methods. Gaussian, Inc., Pittsburgh, PA

Francl MM, Pietro WJ, Hehre WJ, Binkley JS, Gordon MS, DeFrees DJ, Pople JA (1982) Self-consistent molecular-orbital methods. 23. A polarization-type basis set for 2nd row elements. J Chem Phys 77:3654-3665

Fujii T, Suzuki D, Gunjii K, Watanabe K, Moriyama H, Nishizawa K (2002) Nuclear field shift effect in the isotope exchange reaction of chromium(III) using a crown ether. J Phys Chem A 106:6911-6914

Gale JD (2001) Simulating the crystal structures and properties of ionic materials from interatomic potentials. Rev Mineral Geochem 42:37-62

Gale JD, Rohl. AL (2003) The General Utility Lattice Program (GULP). Mol Simul 29:291-341

Galy A, Bar-Matthews M, Halicz L, O'Nions RK (2002) Mg isotopic composition of carbonate: insight from speleothem formation. Earth and Planet Sci Lett 201:1-11

Gao YQ, Marcus RA (2002) On the theory of the strange and unconventional isotopic effects in ozone formation. J Chem Phys 116:137-154

Gillet P, McMillan P, Schott J, Badro J, Grzechnik A (1996) Thermodynamic properties and isotopic fractionation of calcite from vibrational spectroscopy of ^{18}O-substituted calcite. Geochim Cosmochim Acta 60:3471-3485

Gonze X, Beuken J-M, Caracas R, Detraux F, Fuchs M, Rignanese G-M, Sindic L, Verstraete M, Zerah G, Jollet F, Torrent M, Roy A, Mikami M, Ghosez P, Raty J-Y, Allan DC (2002) First-principles computation of material properties: the ABINIT software project. Comput Mat Sci 25:478-492

Hanschmann G (1984) Reduzierte Zustandssummenverhältnisse isotoper Moleküle auf quantenchemischer Grundlage V. Mitt. MNDO-MO-Berechnungen zur ^{28}Si/^{30}Si-, ^{32}S/^{34}S- und ^{35}Cl/^{37}Cl-Substitution. Isotopenpraxis 12:437-439

Harrison NM, Leslie M (1992) The derivation of shell model potentials for $MgCl_2$ from *ab initio* theory. Mol Simul 9:171-174

Hawthorne FC (1988) Mössbauer spectroscopy. Rev Mineral 18:255-340

Hazony Y (1966) Effect of zero-point motion on the Mössbauer spectra of $K_4Fe(CN)_6$ and $K_4Fe(CN)_6 \cdot 3H_2O$. J Chem Phys 45:2664-2668

Heath DF, Linnett JW (1948) Molecular force fields. II. The force fields of the tetrahalides of the group IV elements. Trans Faraday Soc 44:561-568

Heberle J (1971) The Debye integrals, the thermal shift and the Mössbauer fraction. *In*: Mössbauer Effect Methodology, Vol 7. Gruverman IJ (ed), Plenum, p 299-308

Herzberg G (1945) Molecular Spectra and Molecular Structure. II. Infrared and Raman Spectra of Polyatomic Molecules. Von Nostrand Reinhold, New York

Hohenberg P, Kohn W (1964) Inhomogeneous electron gas. Phys Rev 136:B864-871

Horita J, Cole DR, Polyakov VB, Driesner T (2002) Experimental and theoretical study of pressure effects on hydrogen isotope fractionation in the system brucite-water at elevated temperatures. Geochim Cosmochim Acta 66:3769-3788

Housley RM, Hess F (1966) Analysis of Debye-Waller-factor and Mössbauer-thermal-shift measurements. 1. General theory. Phys Rev 146:517-526

Housley RM, Hess F (1967) Analysis of Debye-Waller-factor and Mössbauer-thermal-shift measurements. II. Thermal-shift data on Fe. Phys Rev 164:340-344

Johnson CM, Skulan JL, Beard BL (2002) Isotopic fractionation between Fe(III) and Fe(II) in aqueous solutions. Earth Plan Sci Lett 195:141-153

Kakihana H, Kotaka M, Satoh S, Nomura M, Okamoto M (1977) Fundamental studies on the ion-exchange separation of boron isotopes. Bull Chem Soc Japan 50:158-163

Kieffer SW (1982) Thermodynamics and lattice vibrations of minerals: 5. Applications to phase equilibria, isotopic fractionation, and high-pressure thermodynamic properties. Rev Geophys Space Phys 20:827-849

Kohn W, Sham LJ (1965) Self-consistent equations including exchange and correlation effects. Phys Rev 140: A1133-A1138

Kotaka M, Kakihana H (1977) Thermodynamic isotope effect of trigonal planar and tetrahedral species. Bull Research Lab Nuc Reactors 2:13-29

Kotaka M, Shono T, Ikuta E, Kakihana H (1978) Thermodynamic isotope effect of some octahedral hexahalo complexes. Bull Research Lab Nuc Reactors 3:31-37

Krishnan R, Binkley JS, Seeger R, Pople JA (1980) Self-consistent molecular-orbital methods. 20. Basis set for correlated wave-functions. J Chem Phys 72:650-654

Krouse HR, Thode HG (1962) Thermodynamic properties and geochemistry of isotopic compounds of selenium. Can J Chem 40:367-375

Krynauw GN (1990) The estimation of ν_6 of octahedral XY_6 species. Spectrochim Acta 46A:741-745

Le Roux H, Glasser L (1997) Transferable potentials for the Ti-O system. J Materials Chem 7:843-851

Lindemann FA (1919) Note of the vapor pressure and affinity of isotopes. Philosoph Mag 38:173-181

Lindemann FA, Aston FW (1919) The possibility of separating isotopes. Philosoph Mag 37:523-535

Mayer JE, Mayer MG (1940) Statistical Mechanics. John Wiley & Sons, Inc., New York

McMillan P, Hess AC (1988) Symmetry, group theory and quantum mechanics. Rev Mineral 18:11-62

Müller A, Königer F (1974) Schwingungsspektren von $^{50}CrO_4^{2-}$, $^{53}CrO_4^{2-}$, $Cr^{18}O_4^{2-}$, $^{92}MoO_4^{2-}$, $^{100}MoO_4^{2-}$ und $Ru^{18}O_4^{-}$. Zur Berechnung exakter Kraftkonstanten von Ionen. Spectrochim Acta 30A:641-649

Nakamoto K (1997) Infrared and Raman Spectra of Inorganic and Coordination Compounds. John Wiley & Sons, Inc., New York, NY

O'Neil JR (1986) Theoretical and experimental aspects of isotopic fractionation. Rev Mineral 16:1-40

Oi T (2000) Calculations of reduced partition function ratios of monomeric and dimeric boric acids and borates by the *ab initio* molecular orbital theory. J Nuclear Sci Tech 37:166-172

Oi T, Nomura M, Musashi M, Ossaka T, Okamoto M, Kakihana H (1989) Boron isotopic composition of some boron minerals. Geochim Cosmochim Acta 53:3189-3195

Oi T, Yanase S (2001) Calculations of reduced partition function ratios of hydrated monoborate anion by the *ab initio* molecular orbital theory. J Nuclear Sci Tech 38:429-432

Paneth P (2003) Chlorine kinetic isotope effects on enzymatic dehalogenations. Accounts Chem Res 36:120-126

Patel A, Price GD, Mendelssohn MJ (1991) A computer simulation approach to modeling the structure, thermodynamics and oxygen isotope equilibria of silicates. Phys Chem Min 17:690-699

Polyakov VB (1997) Equilibrium fractionation of the iron isotopes: estimation from Mössbauer spectroscopy data. Geochim Cosmochim Acta 61:4213-4217

Polyakov VB, Mineev SD (2000) The use of Mössbauer spectroscopy in stable isotope geochemistry. Geochim Cosmochim Acta 64:849-865

Pople JA, Binkley Js, Seeger R (1976) Theoretical models incorporating electron correlation. Int J Quantum Chem Y-10(Suppl.):1-19

Pople JA, Scott AP, Wong MW, Radom L (1993) Scaling factors for obtaining fundamental vibrational frequencies and zero-point energies from HF/6-31G* and MP2/6-31G* harmonic frequencies. Israel J Chem 33:345-350

Reid RC, Prausnitz JM, Sherwood TK (1977) The Properties of Gases and Liquids. McGraw-Hill, New York

Richet P, Bottinga Y, Javoy M (1977) A review of hydrogen, carbon, nitrogen, oxygen, sulphur, and chlorine stable isotope fractionation among gaseous molecules. Ann Rev Earth Planet Sci 5:65-110

Roe JE, Anbar AD, Barling J (2003) Nonbiological fractionation of Fe isotopes: evidence of an equilibrium isotope effect. Chem Geol 195:69-85

Roothaan CCJ (1951) New developments in molecular orbital theory. Rev Modern Phys 23:69-89

Rudolph W, Brooker MH, Pye CC (1995) Hydration of the lithium ion in aqueous-solution. J Phys Chem 99: 3793-3797

Russell WA, Papanastassiou DA, Tombrello TA (1978) Ca isotope fractionation on the Earth and other solar system materials. Geochim Cosmochim Acta 42:1075-1090

Schachtschneider JH (1964) Report 231/64. Shell Development Co., Houston, Texas

Schauble EA, Rossman GR, Taylor HP, Jr. (2001) Theoretical estimates of equilibrium Fe-isotope fractionations from vibrational spectroscopy. Geochim Cosmochim Acta 65:2487-2497

Schauble EA, Rossman GR, Taylor HPJ (2003) Theoretical estimates of equilibrium chlorine-isotope fractionations. Geochim Cosmochim Acta 67:3267-3281

Schauble EA, Rossman GR, Taylor HPJ (In review) Theoretical estimates of equilibrium chromium-isotope fractionations. Chem Geol

Schmidt MW, Baldridge KK, Boatz JA, Elbert ST, Gordon MS, Jensen JJ, Koseki S, Matsunaga N, Nguyen KA, Su S, Windus TL, Dupuis M, Montgomery JA (1993) General atomic and molecular electronic-structure system. J Computational Chem 14:1347-1363

Scott AP, Radom L (1996) Harmonic vibrational frequencies: An evaluation of Hartree-Fock, Møller-Plesset, quadratic configuration interaction, density functional theory, and semiempirical scale factors. J Phys Chem 100:16502-16513

Shriver DF (1999) Inorganic Chemistry. W. H. Freeman and Co., New York

Simanouti (Shimanouchi) T (1949) The normal vibrations of polyatomic vibrations as treated by Urey-Bradley field. J Chem Phys 17:245-248

Skulan JL, Beard BL, Johnson CM (2002) Kinetic and equilibrium Fe isotope fractionation between aqueous Fe(III) and hematite. Geochim Cosmochim Acta 66:2995-3015

Skulan JL, DePaolo DJ, Owens TL (1997) Biological control of calcium isotopic abundances in the global calcium cycle. Geochim Cosmochim Acta 61:2505-2510

Stewart JJP (1989a) Optimization of parameters for semiempirical methods. 1. Method. J Computational Chem 10:209-220

Stewart JJP (1989b) Optimization of parameters for semiempirical methods. 2. Applications. J Computational Chem 10:221-264

Thiemens M, Savarino J, Farquhar J, Bao HM (2001) Mass-independent isotopic compositions in terrestrial and extraterrestrial solid and their applications. Accounts Chem Res 34:645-652

Thijssen JM (1999) Computational Physics. Cambridge University Press, Cambridge, UK

Urey HC (1947) The thermodynamic properties of isotopic substances. J Chem Soc (London) 562-581

Urey HC, Greiff LJ (1935) Isotopic exchange equilibria. J Am Chem Soc 57:321-327

Wilson EBJ, Decius JC, Cross PC (1955) Molecular Vibrations: The Theory of Infrared and Raman Vibrational Spectra. Dover, New York

Wong MW (1996) Vibrational frequency prediction using density functional theory. Chem Phys Lett 256: 391-399

Yamaji K, Makita Y, Watanabe H, Sonoda A, Kanoh H, Hirotsu T, Ooi K (2001) Theoretical estimation of lithium isotopic reduced partition function ratio for lithium ions in aqueous solution. J Phys Chem A 105: 602-613

Young ED, Galy A, Nagahara H (2002) Kinetic and equilibrium mass-dependent isotope fractionation laws in nature and their geochemical and cosmochemical significance. Geochim Cosmochim Acta 66:1095-1104

APPENDIX: ANNOTATED BIBLIOGRAPHY OF THEORETICAL EQUILIBRIUM FRACTIONATIONS

A number of theoretical studies of equilibrium stable isotope fractionations in non-traditional systems have been published, including several in journals that may be less familiar to interested geochemists. Here I present an annotated bibliography, which is no doubt incomplete but should provide a good start. To maintain some consistency in the face of the many formats that have been used over the years in reporting theoretically calculated fractionations, most results have been converted to fractionation factors in α_{XR-X} form. One study does not contain tabulated results (Hanschmann 1984), but is worth mentioning because of the quantum-mechanical force-field method used to estimate vibrational frequencies. Most of the theoretical results reproduced here are tabulated at a few representative temperatures. Since fractionation factors are typically nearly linear vs. $1/T^2$, interpolations and extrapolations to higher temperatures made on this basis should be reasonably accurate. In some cases only a selection of the published results are given here, focusing on what appear to be the most relevant substances studied. Although these studies cited here use reasonable methods and appear to be carefully executed, critical evaluation of possible procedural, numerical, and typographical errors is encouraged.

GENERAL STUDIES

Urey and Greiff (1935)

This study is one of the earliest attempts to calculate equilibrium fractionation factors using measured vibrational spectra and simple reduced-mass calculations for diatomic molecules. For the sake of consistency I have converted reported single-molecule partition function ratios to α_{XR-X} units.

	α_{XR-X}		
	273.1 K	**298.1 K**	**600 K**
^{7}Li-^{6}Li			
LiH	1.0284	1.0251	1.0084
Li(g)	1.0000	1.0000	1.0000
^{37}Cl-^{35}Cl			
Cl_2	1.0088	1.0075	1.0020
HCl	1.0050	1.0046	1.0019

Bigeleisen and Mayer (1947)

In this study the authors develop simplified equations relating equilibrium fractionations to mass-scaling factors and molecular force constants. Equilibrium isotopic fractionations of heavy elements (Si and Sn) are predicted to be small, based on highly simplified, one-parameter empirical force-field models (bond-stretching only) of SiF_4, $[SiF_6]^{2-}$, $SnCl_4$, and $[SnCl_6]^{2-}$.

	$\alpha_{XR\text{-}X}$ **300 K**
^{30}Si-^{28}Si	
SiF_4	1.111
$[SiF_6]^{2-}$	1.109
^{120}Sn-^{118}Sn	
$SnCl_4$	1.00256
$[SnCl_6]^{2-}$	1.0028

Urey (1947)

Fractionation factors are calculated using measured vibrational spectra supplemented by simplified empirical force-field modeling (bond-stretching and bond-angle bending force constants only).

	$\alpha_{XR\text{-}X}$				
	273.1 K	**298.1 K**	**400 K**	**500 K**	**600 K**
^{7}Li-^{6}Li					
LiH	1.0281	1.0249	1.0161	1.0113	1.0083
Li(g)	1.0000	1.0000	1.0000	1.0000	1.0000
^{37}Cl-^{35}Cl					
$[ClO_4]^-$	1.0972	1.0847	1.0521	1.0353	1.0253
$[ClO_3]^-$	1.0551	1.0478	1.0291	1.0196	1.0140
ClO_2	1.0360	1.0313	1.0185	1.0130	1.0094
Cl_2	1.0086	1.0074	1.0043	1.0028	1.0019
HCl	1.0050	1.0046	1.0032	1.0024	1.0019
^{81}Br-^{79}Br					
$[BrO_3]^-$	1.0093	1.0080	1.0048	1.0032	1.0022
Br_2	1.0014	1.0012	1.0007	1.0004	1.0003
HBr	1.0009	1.0008	1.0006	1.0004	1.0003

Kotaka and Kakihana (1977)

Fractionation factors are calculated for a large variety of trigonal-planar (XY_3) and tetrahedral (XY_4) molecules and molecule-like complexes, with a particular focus on metal halides. Empirical force-field models (MUBFF) are used to estimate vibrational frequencies for the rarer isotopic forms of the substances studied, and aqueous and crystalline molecule-like species are modeled as gas-phase molecules. In the tabulation below the original equilibrium constants have been converted to fractionation factors ($\alpha_{XR\text{-}X}$).

	$\alpha_{XR\text{-}X}$					
	200 K	**300 K**	**400 K**	**500 K**	**700 K**	**1000 K**
^{30}Si-^{28}Si						
$[Si^{16}O_4]^{4-}$	1.1469	1.0760	1.0459	1.0305	1.0161	1.0081
SiF_4	1.1675	1.0886	1.0544	1.0365	1.0195	1.0098
$Si^{35}Cl_4$	1.0930	1.0455	1.0266	1.0174	1.0090	1.0045
$Si^{79}Br_4$	1.0755	1.0359	1.0207	1.0134	1.0069	1.0034
$Si^{127}I_4$	1.0577	1.0270	1.0155	1.0100	1.0051	1.0025
^{37}Cl-^{35}Cl						
$^{11}BCl_3$	1.0201	1.0100	1.0060	1.0039	1.0021	1.0010
$[^{11}BCl_4]^-$	1.0158	1.0074	1.0043	1.0028	1.0014	1.0007
$^{12}CCl_4$	1.0204	1.0097	1.0057	1.0037	1.0019	1.0009
$^{28}SiCl_4$	1.0178	1.0085	1.0050	1.0032	1.0017	1.0008
$^{76}GeCl_4$	1.0162	1.0076	1.0044	1.0028	1.0015	1.0007
^{76}Ge-^{70}Ge						
GeF_4	1.0744	1.0381	1.0229	1.0151	1.0080	1.0040
$Ge^{35}Cl_4$	1.0447	1.0211	1.0122	1.0079	1.0041	1.0020
$Ge^{79}Br_4$	1.0352	1.0162	1.0092	1.0059	1.0030	1.0015
$Ge^{127}I_4$	1.0271	1.0123	1.0070	1.0045	1.0023	1.0011
^{81}Br-^{79}Br						
$^{11}BBr_3$	1.0036	1.0017	1.0010	1.0007	1.0003	1.0002
$[^{11}BBr_4]^-$	1.0028	1.0013	1.0007	1.0005	1.0002	1.0001
$^{12}CBr_4$	1.0034	1.0016	1.0009	1.0006	1.0003	1.0001
$^{28}SiBr_4$	1.0030	1.0014	1.0008	1.0005	1.0003	1.0001
$^{76}GeBr_4$	1.0027	1.0012	1.0007	1.0004	1.0002	1.0001

Kotaka et al. (1978)

This study uses empirical force-field methods similar to those used by Kotaka and Kakihana (1977), with a focus on octahedral (XY_6) molecules and molecule-like complexes. The reader is cautioned that there appear to be typographical errors in the original tabulation.

	$\alpha_{XR\text{-}X}$					
	200 K	**300 K**	**400 K**	**500 K**	**700 K**	**1000K**
^{30}Si-^{28}Si						
$[SiF_6]^{2-}$	1.1432	1.0719	1.0427	1.0281	1.0147	1.0073
^{50}Ti-^{46}Ti						
$[Ti^{35}Cl_6]^{2-}$	1.0170	1.0078	1.0043	1.0028	1.0014	1.0007
$[Ti^{79}Br_6]^{2-}$	1.0194	1.0088	1.0050	1.0032	1.0016	1.0008
^{76}Ge-^{70}Ge						
$[GeF_6]^{2-}$	1.0895	1.0438	1.0256	1.0167	1.0087	1.0043
$[Ge^{35}Cl_6]^{2-}$	1.0358	1.0164	1.0093	1.0060	1.0031	1.0015
^{104}Ru-^{96}Ru						
RuF_6	1.0731	1.0369	1.0220	1.0145	1.0000	1.0067
^{130}Te-^{120}Te						
TeF_6	1.0598	1.0301	1.0179	1.0117	1.0062	1.0031
$[Te^{35}Cl_6]^{2-}$	1.0093	1.0042	1.0024	1.0015	1.0008	1.0004
$[Te^{79}Br_6]^{2-}$	1.0122	1.0055	1.0031	1.0020	1.0010	1.0005
^{180}Hf-^{174}Hf						
$[Hf^{35}Cl_6]^{2-}$	1.0031	1.0014	1.0008	1.0005	1.0003	1.0001
$[Hf^{79}Br_6]^{2-}$	1.0022	1.0001	1.0005	1.0003	1.0002	1.0001
^{192}Os-^{186}Os						
OsF_6	1.0158	1.0080	1.0047	1.0031	1.0016	1.0008
$[Os^{35}Cl_6]^{2-}$	1.0076	1.0035	1.0020	1.0013	1.0006	1.0003
^{193}Ir-^{191}Ir						
IrF_6	1.0062	1.0031	1.0019	1.0012	1.0006	1.0003
$[Ir^{35}Cl_6]^{2-}$	1.0017	1.0008	1.0004	1.0003	1.0002	1.0001
^{198}Pt-^{192}Pt						
PtF_6	1.0208	1.0106	1.0063	1.0042	1.0022	1.0011
$[PtF_6]^{2-}$	1.0092	1.0044	1.0026	1.0017	1.0009	1.0004
$[Pt^{35}Cl_6]^{2-}$	1.0049	1.0023	1.0013	1.0008	1.0004	1.0002
$[Pt^{79}Br_6]^{2-}$	1.0054	1.0024	1.0014	1.0009	1.0004	1.0002

Hanschmann (1984)

S, Cl and Si-isotope fractionations for gas-phase molecules and aqueous molecule-like complexes (using the gas-phase approximation) are calculated using semi-empirical quantum-mechanical force-field vibrational modeling. Model vibrational frequencies are not normalized to measured frequencies, so calculated fractionation factors are somewhat different from fractionations calculated using normalized or spectroscopically determined frequencies. There is no table of results in the original publication.

Bochkarev et al. (2003)

Li, Mg and Cl-isotope fractionations for gas-phase molecules and aqueous molecule-like complexes (using the gas-phase approximation) are calculated using *ab initio* vibrational modeling. The results below are calculated using Hartree-Fock quantum mechanical modeling. Model frequencies have not been normalized to spectroscopically measured frequencies, resulting in a probable overestimate of fractionation factors—compared for instance with Urey (1947). For consistency, results have been converted from the original format (lnβ) to $\alpha_{XR\text{-}X}$.

	$\alpha_{XR\text{-}X}$ **300 K**
^{7}Li-^{6}Li	
LiH	1.0252
LiF	1.0761
^{26}Mg-^{24}Mg	
MgO	1.0164
MgH	1.0041
MgF	1.0148
^{37}Cl-^{35}Cl	
$[ClO_4]^-$	1.0934
$[ClO_3]^-$	1.0637
ClO_2	1.0423
Cl_2	1.0087
HCl	1.0050
NaCl	1.0024
LiCl	1.0030

ELEMENT-SPECIFIC STUDIES

Lithium

Yamaji et al. (2001)

Fractionation factors for Li-H_2O clusters are calculated using *ab initio* vibrational models, in the gas-phase approximation. Vibrational frequencies in this system are largely unknown, and the few that have been measured are contentious. In the absence of reliable experimental constraints, Hartree-Fock model *ab initio* vibrational frequencies are normalized using a scaling factor of 0.8964. It is generally thought that aqueous lithium is coordinated to four water molecules (Rudolph et al. 1995). The authors speculate that 6-coordinate lithium in adsorbed or solid phases will have lower $^{7}Li/^{6}Li$ than coexisting aqueous Li^{+}.

	$\alpha_{XR\text{-}X}$ **298 K**
^{7}Li-^{6}Li	
$[Li(H_2O)_4]^{+}$	1.064
$[Li(H_2O)_4]^{+}\bullet 2H_2O$	1.072

Chromium

Schauble et al. (in press)

Fractionations (β-factors) calculated for aqueous molecule-like complexes and anhydrous crystalline Cr-metal and Cr_2O_3, using multiple empirical and *ab initio* force-field vibrational models as well as measured vibrational spectra of isotopically substituted species. Only best-estimate results are listed here. The authors predict high $^{53}Cr/^{52}Cr$ ratios in oxidized $[CrO_4]^{2-}$ relative to Cr^{3+}-bearing species like $[Cr(H_2O)_6]^{3+}$ and Cr_2O_3, and lower $^{53}Cr/^{52}Cr$ in species with Cr-N or Cr-Cl bonds than in structurally similar species with Cr-O bonds. The results also suggest a strong correlation between short bond lengths and high $^{53}Cr/^{52}Cr$ ratios at equilibrium.

	$\alpha_{XR\text{-}X}$			
	273.15 K	**298.15 K**	**373.15 K**	**573.15 K**
^{53}Cr-^{52}Cr				
$[CrCl_6]^{3-}$	1.0040	1.0034	1.0022	1.0009
$[Cr(NH_3)_6]^{3+}$	1.0061	1.0052	1.0034	1.0015
$[Cr(H_2O)_6]^{3+}$	1.0080	1.0069	1.0045	1.0020
$[CrO_4]^{2-}$	1.0156	1.0135	1.0092	1.0042
Cr-Metal	1.0041	1.0034	1.0022	1.0009
Cr_2O_3	1.0076	1.0065	1.0043	1.0019

Chlorine

Schauble et al. (2003)

Fractionations for gas-phase molecules and aqueous perchlorate (gas-phase approximation) calculated using *ab initio* force-field vibrational models normalized to measured frequencies. Fractionation factors are also calculated for crystalline chlorides using empirical force fields. Includes an indirect model of aqueous Cl^- ($\alpha_{Cl-(aq)-Cl} \approx 1.0021–1.0030$ at 295K) based on measured NaCl–Cl^-(aq) and KCl–Cl^-(aq) fractionations (Eggenkamp et al. 1995) and the theoretically estimated α_{XR-X} for NaCl and KCl.

	α_{XR-X}									
	153 K	**173 K**	**193 K**	**233 K**	**273 K**	**298 K**	**373 K**	**473 K**	**673 K**	**1273 K**
^{37}Cl-^{35}Cl Molecules										
Cl_2	1.0227	1.0187	1.0157	1.0114	1.0087	1.0074	1.0049	1.0031	1.0016	1.0005
HCl	1.0099	1.0087	1.0077	1.0062	1.0052	1.0047	1.0036	1.0027	1.0017	1.0006
C_2Cl_4	1.0334	1.0273	1.0227	1.0164	1.0124	1.0106	1.0070	1.0045	1.0023	1.0007
C_2HCl_3	1.0310	1.0254	1.0213	1.0154	1.0117	1.0100	1.0067	1.0043	1.0022	1.0006
CCl_3F	1.0337	1.0274	1.0228	1.0163	1.0123	1.0104	1.0069	1.0044	1.0022	1.0006
CCl_4	1.0325	1.0264	1.0218	1.0156	1.0117	1.0099	1.0065	1.0041	1.0021	1.0006
$CHCl_3$	1.0294	1.0241	1.0201	1.0146	1.0110	1.0094	1.0063	1.0040	1.0020	1.0006
CH_2Cl_2	1.0267	1.0221	1.0187	1.0138	1.0106	1.0091	1.0061	1.0040	1.0020	1.0006
CH_3Cl	1.0243	1.0205	1.0175	1.0131	1.0102	1.0088	1.0060	1.0039	1.0020	1.0006

	273 K	**298 K**	**373 K**	**573 K**
Crystals				
NaCl	1.0039	1.0033	1.0021	1.0009
KCl	1.0030	1.0025	1.0016	1.0007
RbCl	1.0028	1.0023	1.0015	1.0006
$FeCl_2$	1.0067	1.0056	1.0036	1.0015
$MnCl_2$	1.0062	1.0052	1.0034	1.0014

Iron

Polyakov (1997), Polyakov and Mineev (2000)

$^{57}Fe/^{54}Fe$ fractionations (β-factors) are calculated for a range of iron-bearing minerals and crystal phases by modeling Mössbauer spectroscopic data. The ability of Mössbauer methods to characterize trace amounts of iron allows modeling of solid-solution effects and complex mineral species. The authors predict measurable fractionations between common mineral species, including a general enrichment of heavy iron isotopes in Fe^{3+} bearing minerals. Selected results from the more recent paper are reproduced here—these appear to recapitulate the earlier results. Results are tabulated in the form of a polynomial expansion vs. inverse temperature,

$$1000 \bullet \ln\alpha_{XR\text{-}R} = B_1x - B_2x^2 + B_3x^3,\ x = 10^6/T^2$$

^{57}Fe-^{54}Fe	B_1	B_2	B_3
Iron metal	0.69964	0.001476	0.000004845
Hematite Fe_2O_3	0.98684	0.002937	0.000013597
Magnetite Fe_3O_4 (A site)	1.74563	0.009190	0.000075260
(B site)	1.28250	0.004961	0.000029846
Goethite FeOOH	0.78168	0.001843	0.000006758
Akaganeite FeOOH (A site)	1.35089	0.005504	0.000034880
(B site)	0.94776	0.002709	0.000012050
Lepidocrocite FeOOH	0.72987	0.001607	0.000005501
Spinel $Mg_{0.9}Fe_{0.1}Al_2O_4$	0.45632	0.000628	0.000001344
Ilmenite $FeTiO_3$	0.37934	0.000434	0.000000772
Ferrochromite $FeCr_2O_4$	0.42987	0.000557	0.000001124
Periclase MgO:Fe	0.60395	0.001087	0.000003062
Diopside $Ca_{1.03}Mg_{0.64}Fe_{0.31}Si_{1.94}O_6$ (A site)	1.17247	0.004146	0.000022804
(B site)	0.48355	0.000705	0.000001560
Hedenbergite $CaMg_{0.15}Mn_{0.03}Fe_{0.76}Al_{0.03}Si_3O_6$	0.46984	0.000666	0.000001467
Aegirine $NaFeSi_2O_6$	1.15105	0.003996	0.000021577
Enstatite $Mg_{1.95}Fe_{0.05}Al_{0.05}Si_{1.96}O_6$ (A site)	0.49747	0.000746	0.000017420
(B site)	0.49747	0.000746	0.000017420
Enstatite $Mg_{1.65}Fe_{0.27}Al_{0.03}Si_{2.02}O_6$ (A site)	0.42987	0.000557	0.000001124
(B site)	0.66355	0.001328	0.000004134
Olivine $(Mg,Fe)_2SiO_4$	0.57000	0.000980	0.000002620
Monoclinic Chloritoid $Al_{1.98}Fe_{0.94}Mn_{0.10}SiO_5(OH)_2$	0.42987	0.000557	0.000001124
Triclinic Chloritoid $Al_{1.95}Fe_{0.75}Mn_{0.23}Mg_{0.13}SiO_5(OH)_2$	0.45632	0.000628	0.000001344
Pyrite FeS_2	1.46882	0.006506	0.000044835
Nickel Sulfide $Ni_{1-x}Fe_xS_2$	1.23789	0.004621	0.000026839
Ankerite $CaFe_{0.5}Mg_{0.5}(CO_3)_2$	0.35526	0.000381	0.000000634
Ankerite $Ca_{1.1}Fe_{0.3}Mg_{0.5}Mn_{0.1}(CO_3)_2$	0.48355	0.000705	0.000001560
Siderite $FeCO_3$	0.55510	0.000929	0.000002420

Schauble et al. (2001)

$^{56}Fe/^{54}Fe$ fractionations (β-factors) are calculated for aqueous molecule-like complexes, using empirical force-field (MUBFF) vibrational models. Materials studied include Fe-H_2O and Fe-Halide complexes with tetrahedral and octahedral geometries, cyano-complexes, and iron metal. These calculations predict measurable fractionations between aqueous species, governed by the oxidation state of iron (Fe^{3+} – high $^{56}Fe/^{54}Fe$, Fe^{2+} – low $^{56}Fe/^{54}Fe$), and covalent bonding strength of bond partners (CN^-, H_2O – high $^{56}Fe/^{54}Fe$, Cl^-, Br^- – low $^{56}Fe/^{54}Fe$). The calculations also suggested significant coordination-number effects (4-fold coordination – high $^{56}Fe/^{54}Fe$, 6-fold coordination – low $^{56}Fe/^{54}Fe$). Results for Fe-metal and ferrocyanide complexes (not shown here) generally agree with earlier Mössbauer-based models (Polyakov 1997; Polyakov and Mineev 2001).

	$\alpha_{XR\text{-}X}$				
	273.15 K	**298.15 K**	**373.15 K**	**473.15 K**	**573.15 K**
^{56}Fe-^{54}Fe					
$[Fe(H_2O)_6]^{3+}$	1.0137	1.0117	1.0076	1.0048	1.0033
$[FeCl_4]^-$	1.0085	1.0072	1.0047	1.0029	1.0020
$[FeBr_4]^-$	1.0076	1.0064	1.0041	1.0026	1.0018
$[Fe(H_2O)_6]^{2+}$	1.0073	1.0062	1.0040	1.0025	1.0017
Fe-metal	1.0063	1.0053	1.0034	1.0021	1.0015
$[FeCl_4]^{2-}$	1.0048	1.0040	1.0026	1.0016	1.0011
$[FeCl_6]^{3-}$	1.0046	1.0038	1.0025	1.0015	1.0011

Anbar et al. (in press)

$^{56}Fe/^{54}Fe$ fractionations (β-factors) are calculated for the aqueous Fe^{2+} and Fe^{3+} complexes $[Fe(H_2O)_6]^{2+}$ and $[Fe(H_2O)_6]^{3+}$, using hybrid density functional theory (DFT). *Ab initio* model frequencies are not scaled. The high electric charge of these complexes and the strong tendency of bonded water molecules to form hydrogen bonds can make gas-phase models of aquo-complexes like these inaccurate. Anbar et al. correct for these effects using an implicit model of the bulk solvent. In the implicit solvation models, the solvent (i.e., water not directly bonded to the central metal cations) is treated as a polarizable, dielectric continuum. This polarizable continuum model (PCM) improves the match between model and experimental molecular structures and vibrational frequencies, and probably yields more reliable fractionation estimates. However, there is still substantial disagreement (>100 cm^{-1}) with measured O-Fe-O bending frequencies in $[Fe(H_2O)_6]^{3+}$, possibly suggesting an error in the original spectroscopic interpretation. Calculated fractionations involving $[Fe(H_2O)_6]^{3+}$ appear to agree more closely with experiments than the MUBFF-based calculation of Schauble et al. (2001), mainly because of the different O-Fe-O vibrational frequencies used by these authors.

	$\alpha_{XR\text{-}X}$						
	273 K	**283 K**	**298 K**	**323 K**	**373 K**	**473 K**	**573 K**
^{56}Fe-^{54}Fe							
DFT (PCM solvent)							
$[Fe(H_2O)_6]^{3+}$	1.0108	1.0101	1.0092	1.0079	1.0060	1.0038	1.0026
$[Fe(H_2O)_6]^{2+}$	1.0079	1.0074	1.0067	1.0058	1.0044	1.0028	1.0019
DFT (gas phase)							
$[Fe(H_2O)_6]^{3+}$	1.0112	1.0104	1.0095	1.0082	1.0062	1.0040	1.0028
$[Fe(H_2O)_6]^{2+}$	1.0077	1.0072	1.0066	1.0057	1.0043	1.0028	1.0019

Selenium

Krouse and Thode (1962)

Fractionations are calculated for a number of gas-phase molecules and aqueous ions (treated as gases) using measured vibrational spectra and empirical force field calculations.

	$\alpha_{XR\text{-}X}$			
	273.15 K	**298.15 K**	**373.15 K**	**523.15 K**
^{82}Se-^{76}Se				
SeF_6	1.059	1.051	1.034	1.019
$[SeO_4]^{2-}$	1.044	1.038	1.023	1.014
Se_2	1.012	1.011	1.007	1.004
SeO(g)	1.009	1.008	1.005	1.003
H_2Se(g)	1.005	1.005	1.003	1.002
PbSe(g)	1.005	1.004	1.003	1.001
Se^-(g)	1.000	1.000	1.000	1.000